

¹⁴C DATES AND THE IRON AGE CHRONOLOGY OF ISRAEL: A RESPONSE

Amihai Mazar

Institute of Archaeology, The Hebrew University of Jerusalem, Israel. Corresponding author. Email: mazar@huji.ac.il.

Christopher Bronk Ramsey

University of Oxford, Research Laboratory for Archaeology and the History of Art, Dyson Perrins Building, South Parks Road, Oxford, OX1 3QY, United Kingdom.

ABSTRACT. Boaretto et al. (2005) published 68 radiocarbon dates relating to 30 samples from 10 Iron Age sites in Israel as part of their Early Iron Age Dating Project. Though the main goal of their paper was an interlaboratory comparison, they also presented results of Bayesian models, calculating the transition from Iron Age I to Iron Age II in Israel to be about 900 BCE instead of the conventional date of about 1000 BCE. Since this date has great importance for all of Eastern Mediterranean archaeology, in this paper we examine the results in light of the dates published in the above-mentioned article. Our paper was revised in light of new data and interpretations published by Sharon et al. (2007).

Following a survey of the contexts and specific results at each site, we present several Bayesian models. Model C2 suggests the date range of 961–942 BCE (68% probability) for the transition from Iron Age I to Iron Age II, while Model C3 indicates a somewhat later date of 948–919 BCE (compare the date 992–961 BCE calculated at Tel Rehov for the same transition). In our Model D, we calculated this transition date at Megiddo as taking place between 967–943 BCE. Finally, we calculated the range of dates of major destruction levels marking the end of the Iron Age I, with the following results: Megiddo VIA: 1010–943 BCE; Yoqne'am XVII: 1045–997 BCE; Tell Qasile X: 1039–979 BCE; Tel Hadar: 1043–979 BCE (all in the 68.2% probability range). Figure 4 indicates that the transition between Iron I and II probably occurred between these above-mentioned destruction events and the dates achieved in our Models C2 or C3, namely during the first half of the 10th century BCE.

This study emphasizes the sensitivity of Bayesian models to outliers, and for reducing or adding dates from the models. This sensitivity should be taken into account when using Bayesian models for interpreting radiometric dates in relation to subtle chronological questions in historical periods.

Abbreviations used in this paper:

GrA: samples measured at the Centre for Isotope Research (CIO), University of Groningen (the Netherlands) by accelerator mass spectrometry (AMS).

GrN: samples measured at the CIO, University of Groningen using proportional gas counting.

HC: High Chronology. Meaning the conventional chronology as presented in Stern (1993), utilized by Mazar (1990) and others; Iron I: 1200–1000 BCE; Iron IIA: 1000–900; Iron IIB: 900–700.

LC: Low Chronology, as suggested by Finkelstein (1996) and elaborated by Gilboa and Sharon (2001, 2003). The LC dates the transition between the Iron I to Iron II to about 900 BCE and the transition between Iron IIA and Iron IIB to about 800 BCE.

LSC: samples prepared and measured at Rehovot (Israel) in liquid scintillation counters, followed by the sample number of the Early Iron Age Dating Project.

MCC: Modified Conventional Chronology (Mazar 2005). Iron I: 1200–980 BCE; Iron IIA: about 980–840/830 BCE.

RTT: samples prepared at the Weizmann Institute in Rehovot and measured in Tucson (Arizona, USA) by the AMS method, followed by the sample number of the Early Iron Age Dating Project.

T: samples prepared and measured in Tucson by the AMS method, followed by the Tucson laboratory number.

LBA: the Late Bronze Age.

Site codes:

A = Aphek; **BD** = Bethsaida; **D** = Tel Dor; **HD** = Tel Hadar; **HM** = Tell el-Hammah; **HB** = Hebron (Tell el-Rumeideh); **HZ** = Hazor; **K** = Tell Keisan; **MG** = Megiddo; **MQ** = Tel Miqne; **NE** = Nahal 'Elah; **NH** = Negev Highlands; **QS** = Tell Qasile; **R** = Tel Rehov; **RZ** = Horbat Rosh Zayit; **SH** = Shiloh; **SF** = Tell es-Safi; **Y** = Yoqne'am.

INTRODUCTION

The chronology of the Iron Age I–IIA in Israel (12th to late 9th centuries BCE) has been the subject of ongoing debate since 1995–1996, when Finkelstein (1996) suggested a Low Chronology (LC), which is lower by 60–100 yr than the conventional High Chronology (HC). This debate has far-reaching implications for the archaeology and historical interpretation of the Iron Age in the Levant, as well as for the archaeological chronology of Greece and Cyprus in the Iron Age, which depends on that of the Levant (for summaries and earlier bibliography, see Finkelstein 2005; Mazar 2005). The attempts to utilize radiocarbon dates in resolving this debate have already produced substantial literature, culminating in the publication of a conference dedicated to this subject (Levy and Higham 2005). One prominent project was carried out on samples from Tel Rehov in northern Israel, where about 100 dates are now available. About 40 of these samples were measured in the late 1990s at the Weizmann Institute of Science at Rehovot and at the Tucson University laboratories (Mazar and Carmi 2001), while another 64 were measured at the Groningen laboratory (Bruins et al. 2005a; Mazar et al. 2005; van der Plicht and Bruins 2005).¹ A second batch of dates, measured at the Weizmann Institute in the 1990s, comes from Tel Dor (Gilboa and Sharon 2001, 2003). The Early Iron Age Dating Project led by Boaretto, Gilboa, Jull, and Sharon (Boaretto et al. 2005; Sharon et al. 2005, 2007) set as its objective to obtain as many ¹⁴C determinations as possible from Iron I–IIA sites in Israel measured at different laboratories, and in this way, attempts to resolve the chronological debate. Since this project is of the utmost importance to our field, we find it interesting to examine the results published so far, and in particular to evaluate the conclusion that the transition from Iron I to Iron IIA occurred about 900 BCE. We would like to express our appreciation of this highly important project, which enables such a unique comprehensive study of radiometric dates relating to a crucial archaeological and historical era.

Boaretto et al. (2005) published 68 dates from 10 different sites measured at Rehovot (LSC) or Tucson (T) or prepared at Rehovot and measured at Tucson (RTT). The same samples were measured by 2 or even 3 different methods, thus enabling interlaboratory comparisons. In an initial version of the present paper, we examined the results of the Bayesian models as published by Boaretto et al. (2005) and presented alternative models based on evaluation of the same data combined with a few additional dates. After the submission of that paper in March 2007, a more detailed report on the Iron Age Dating Project including additional radiometric dates, calibrated dates, and Bayesian models was published in this journal by Sharon et al. (2007). In the present version of our paper, we added dates published by Sharon et al. (2007), as well as a few additional dates from Megiddo and Shiloh also measured by Boaretto and others in the framework of their project, but published elsewhere as specified below. We also added an additional date from Tell Qasile measured at Groningen (QS5 in Table 3) and 2 dates from an Iron IIA context in the Negev Highlands. However, since our initial paper was written before the appearance of Sharon et al. (2007), we retained the original structure of our tables and the averages as cited from Boaretto et al. (2005) and Boaretto (2006), even though in some cases they were slightly different from those presented by Sharon et al. (2007).

¹The introductory chapter in Mazar (2005) and 3 papers on the Tel Rehov ¹⁴C dates—van der Plicht et al. (2005); Mazar et al. (2005); Bruins et al. (2005a)—are available as PDF files at www.rehov.org.

Exceptions are marked in the comments to the tables. Table 2a shows the dates of charred timber from Megiddo Stratum VIA measured at the Weizmann Institute in the late 1990s and published in the Megiddo reports (see the Table 2a footnote for references). We excluded from this study the 64 Groningen dates from Tel Rehov published by Mazar et al. (2005), as well as the dates from Tel Dor obtained at the Weizmann Institute in the late 1990s, since both were discussed in detail in the publications mentioned above. We also omit in this study several other Iron I–IIA ¹⁴C dates.² Thus, the following discussion is based on only part of the available measured dates from this period. It should also be taken into account that the Iron Age Dating Project is currently in its second phase, and thus an additional large amount of data is expected to be published in the near future. Future studies will have to combine all the available data concerning this period. We did not include in our tables calibrated dates (most of these are presented in Sharon et al. 2007: Table 8).

It should be noted that while in Boaretto et al. (2005) Tucson and Rehovot laboratory numbers were marked as separate sample numbers, the same dates were marked in Sharon et al. (2007) as sample numbers of the Iron Age Dating Project. We present in our tables both numbering systems in 2 different columns. In our tables, each laboratory is presented separately, as in Boaretto et al. (2005), and we added codes of our own to each sample from each laboratory (composed of a letter code for the site and running numbers for individual samples or for part of the samples measured separately by different methods). It should be noted that all dates with similar sample numbers in Sharon et al. (2007) come from the same sample of seeds or charcoal, even though they may appear in several lines in our tables since they were measured by different methods. When such clusters pass the χ^2 test and are all done by 1 laboratory, we used the average date as calculated by Boaretto et al. (2005) or Sharon et al. (2007).

We arranged the data in 3 tables:

Table 1: dates from the end of the Late Bronze Age and Iron I contexts

Table 2: dates from contexts attributed to the end of Iron I

Table 2a: dates of charred beams from Megiddo VIA

Table 3: dates from Iron IIA contexts (both from destruction layers from the end of the period as well as occupation layers that represent the duration of the period)

Our Bayesian models A–D (Figure 1) present the results. Models A1–A2 are based solely on data published by Boaretto et al. (2005), while our Models B1–B2 and C1–C3 incorporate also the additional dates mentioned above, in various combinations. Model D refers to dates from Megiddo alone. Figure 3 shows the dates of 4 destruction layers attributed to the end of the Iron Age I.

²In the present study, we did not include dates from the following sites: Khirbet en-Nahas (Higham et al. 2005), since the pottery is not yet published; dates from Tel Hadar mentioned by Finkelstein and Piasezky (2005:295–296), since they supply only an average of 11 unpublished dates; dates from Tel Dan (Bruins et al. 2005b), since most of them (except one) are of charcoal and the context might be controversial (Finkelstein and Piasezky 2006b; though it seems that their criticism is much exaggerated); el-Akhwat (Iron Age I) and Sulem (Iron IIA) published in Sharon et al. (2007:25, 35), since pottery from these sites was not yet published; Beth Shemesh, since sample 3987 (Sharon et al. 2007:44) is from an insecure context (either Stratum 4 of late Iron I or Stratum 3 of early Iron IIA). We also did not include several Iron Age I contexts published by Sharon et al. (2007) (samples 4525 and 4528 from Dor and samples 4286 and 4283 from Tel Miqne), which were not mentioned by Boaretto et al. (2005) and thus were not included in the original version of this paper, since our emphasis was on the late Iron I and Iron IIA transition. These samples would not change our results.

THE END OF THE LATE BRONZE AGE AND THE SPAN OF THE IRON AGE I (TABLE 1)

Table 1 includes dates from contexts belonging to the end of the Late Bronze Age and to Iron Age I (the latter dated conventionally to 1200–1000 BCE), not including dates that definitely come from the end of the period; the latter are assembled in Table 2.

Table 1 The end of the Late Bronze Age and the span of Iron Age I.

Site+stratum	Sample	Lab # (Boaretto et al. 2005)	Sample # (Sharon et al. 2007)	Code in present paper	¹⁴ C BP date or average of several dates
Megiddo K-6 (VIIA?) ^a	Olive stones	T-18169a, aa	4499a, aa	MG1	2893 ± 27
		RTT-4499.3 1.1–3	4499.3–5	MG2	2894 ± 23
		T-18170a, aa	4500a, aa	MG3	2968 ± 30
		RTT-4500.3 1.1–3	4500.3–5	MG4	2918 ± 22
Tell Keisan 13	Charcoal	T-18158a, aa	3804a, aa	K1	2999 ± 29
		RTT-3804.3–5	3804.3–5	K2	2984 ± 20
Hazor XII/XI	Charcoal	AA-40992	3700a	HZ1	2945 ± 50
		AA-40993	3701a	HZ2	2965 ± 50
	Olive stones	AA-40994	3702a	HZ3	3060 ± 50
		Charcoal	AA-40995	3703a	HZ4 ^b
	Charcoal	AA-40996	3704a	HZ5 ^b	3370 ± 60
		RTT-3700	3700.3	HZ6	2975 ± 35
	Olive stones	RTT-3701	3701.3	HZ7	2940 ± 30
		RTT-3702	3702.3	HZ8	3060 ± 30
	Charcoal	RTT-3703	3703.3	HZ9 ^b	3570 ± 53
		RTT-3704	3704.3	HZ10 ^b	3375 ± 30
Tel Hebron	Charcoal	LSC-4148.1	4148.1	HB1	3010 ± 35
		RTT-4148.3–5	4148.3–5	HB2	2998 ± 23
Tel Miqne V ^c	Olive stones	T-18168a, aa	4282a, aa	MQ1	2883 ± 26
		RTT-4282.3–5	4282.3–5	MQ2	2872 ± 27
Tel Rehov D-4 ^d Locus 1836	Olive stones	RTT-3809.4–5	3809.4–5	R1	2845 ± 25
		T-18150a, aa	3809a, aa	R2	2913 ± 45
Shiloh V ^e	Grain Area D	LSC [# not provided]	?	SH1	2868 ± 20
	Grain, Area D	RTT [# not provided]	3927	SH2	2854 ± 25
	Raisins, Area C	RTT [# not provided]	3928.3–5	SH3	2897 ± 23
	Seeds, Area C	RTT [# not provided]	3929.3–5	SH4	2959 ± 28

^aWe omit sample 4501.1–3 (Sharon et al. 2007:24) as it is much too low. The calibrated date of 10/9th centuries BCE for this sample is an unreasonable date for Stratum VIIA at Megiddo.

^bDates of early wood from Hazor (see comments below).

^cSee comments below and in Footnote 3.

^dCompare dates published from Groningen in Mazar et al. (2005:199).

^eThe dates SH2–SH4 are cited from Sharon et al. (2007). Note that SH2 is mentioned in their Table 8, but not in their Table 7. SH1 is cited from Finkelstein and Piasezky (2006a:46) (not mentioned by Sharon et al. 2007).

Megiddo VIIA (=K-6 in the Tel Aviv University excavations) and Tell Keisan 13. According to conventional archaeological dating, these contexts belong to the 12th century BCE. The ¹⁴C dates from both sites indeed cover the entire or parts of the 12th century, as well as a range of dates on both sides of this century, due to the shape of the calibration curve for this period. Three samples of olive stones from Megiddo K-6 are available. Sample 4499 (MG1 and MG2) is somewhat too low (calibrated date 1120–1049 BCE, 68% probability) if indeed Level K-6 of the Tel Aviv University excavations is contemporary with Stratum VIIA of the Chicago excavations, since the latter is supposed to be no later to the end of the Egyptian hegemony in Canaan at about 1130 BCE (Finkelstein et al. [2006:17] correlate Level K-6 to “Stratum VIIA or slightly later”). Sample 4500 (MG4) would fit this historical date, while sample 4501 is omitted by us since it is unreasonably low (see Footnote a in Table 1). The single sample from Tell Keisan (3804) is of charcoal and has a wide calibrated range (1270–1130 BCE) and thus is of less importance.

Hazor XII/XI. These samples come from Iron I pits cut into Late Bronze occupation strata. The single short-lived sample 3702 (HZ3 and HZ8) is dated to the 14th–13th centuries BCE, a surprisingly early date for this context. It is hard to believe that these olive stones are residual; thus, this sample may hint to an earlier date than the traditional 12th–11th centuries BCE date of Hazor Stratum XII (Ben-Ami 2001). The other 4 samples are of charcoal: 2 are certainly from old wood (dated to the Middle Bronze Age!), while the other 2 could be contemporary with the short-lived sample 3702. Interestingly, none of these dates is later than the 13th century BCE.

Tel Hebron. The dates of the charcoal sample 4147 from an Iron I context, as well as an additional similarly dated charcoal (4148, not included in our Table 1, see Sharon et al. 2007:26, 41) is in the range of the 14th–12th centuries BCE. The old-wood effect probably exists here, though the 12th century date may fit the (as yet unpublished) archaeological evidence.

Tel Miqne - Ekron Stratum V. The dates of sample 4282 fit the conventional date of Stratum V in the mid or second half of the 11th century BCE.³

Shiloh. The 3 or 4 samples of seeds and raisins come from the destruction of Shiloh Stratum V (Finkelstein and Piasezky 2006a:46; Sharon et al. 2007:26, 41). It is unknown whether this violent destruction occurred at the end of the Iron Age I or somewhat earlier, and therefore we included these dates in our Table 2. Historical considerations led to a date of ~1050 BCE (Finkelstein 1993:389) and this may fit samples 3927 and 3928 (SH1–2) as well as SH3, while sample 3929 (SH4) is much too early (calibrated in the 68% range to 1260–1120 BCE; only the lowest end of the 95% range, 1050 BCE, may fit the historical dating).

Tel Rehov. The dates of sample 3809 (R1 and R2) from Tel Rehov Stratum D-4 confirm the dates measured at Groningen (Mazar et al. 2005:207).

Conclusion. The Iron Age I dates mentioned above either fit the HC or are too early (in the case of Hazor). None indicate continuity of the Iron Age I into the 10th century BCE as suggested by the LC.

³Sample 4282 (=MQ1–2) was published by Boaretto et al. (2005) as belonging to Tel Miqne Stratum IV; in Sharon et al. (2007:27) it was marked as “Stratum Vb (or IV??).” S. Gitin clarified to us that the sample came from Stratum V. We did not include in our tables sample 4286 from Stratum VIIB, a context that is essential for the debate concerning the date of the earliest Philistine settlement. The calibrated date of this sample (Sharon et al. 2007:24, 41) between 1190–1030 at 68% probability may fit both the excavator’s and Mazar’s date 1180–1140/30 BCE (during the time of the Egyptian 20th Dynasty) as well as Ussishkin and Finkelstein’s lower dates (1140/30–1200 BCE) and thus does not help to resolve this debate.

THE END OF IRON AGE I (TABLE 2)

The date of the end of the Iron Age I is the most controversial issue relating to the Iron Age chronological debate; suggested dates are between 1000/980 (conventional dating and MCC) and about 900 BCE (LC; Sharon et al. 2007), hence the importance of dates from 5 destruction layers that are reliable, primary contexts and agreed by all archaeologists of the Levant as representing the end of the Iron Age I. These include Megiddo Stratum VIA (Level K-4 in the Tel Aviv University excavations); Yoqne'am Stratum XVII, which yielded material culture identical to that of Megiddo VIA; Tell Keisan Stratum 9a; Tell Qasile Stratum X; and Tel Hadar Stratum IV. To these, we added dates from Tel Dor phases 9–10 in Area D2 and Tel Rehov Stratum D-3 pits (for the latter, only those dates mentioned by Boaretto et al. 2005 and Sharon et al. 2007). The 2 latter contexts are not from destruction layers; Tell el-Hammah “lower” is also mentioned here, though we have reservations concerning its attribution to the late Iron I period (see below).

Table 2 The end of Iron Age I.

Site	Sample	Lab # (Boaretto et al. 2005 or Boaretto 2006)	Sample # (Sharon et al. 2007)	Code # in present paper	¹⁴ C BP date or average of several dates ^a	
Megiddo VIA (=K4) destruction	Seeds	RTT-3944.3–5	3944.3–5	MG5	2957 ± 31 ^b	
		T-18163a	3944a	MG6	2864 ± 40 ^b	
Megiddo VIA (=K4) (“pre-destruction”)	Olive stones	RTT-3945a, aa	3945a, aa	MG7	2880 ± 30	
		RTT-3946a, aa	3946a, aa	MG8	2910 ± 25	
Megiddo VIA (=K4) destruction		RTT-3939.3–5		MG9	2804 ± 24 ^c	
		RTT-3940.3–5	3940.3–5	MG10	2765 ± 25	
		RTT-3942.3–6	3942.3–6	MG11	2845 ± 25	
		RTT-3943.4–5	3943.3–5	MG12	2855 ± 25	
Yoqne'am XVII 3777: Locus 3042 3778: Locus 3047 3779: Locus 3035	Seeds	LSC-3777.1	3777.1	Y1	2866 ± 25	
		RTT-3777.3–5	3777.3–5	Y2	2866 ± 33	
		LSC-3778.1	3778.1	Y3	2776 ± 25	
		RTT-3778.3–5	3778.3–5	Y4	2817 ± 26	
		T-18150a, aa	3778a, aa	Y5	2818 ± 29	
		Same locus as sample 3778 ^d	GrA-255534	Y11	2925 ± 38	
			GrA-25708	Y12	2897 ± 38	
			GrA-25767	Y13	2929 ± 54	
		LSC-3779.1	3779.1	Y6	2926 ± 30	
		RTT-3779.3–5	3779.3–5	Y7	2824 ± 30	
Tell Keisan 9a–b	Charcoal	T-18157a, aa	3803a, aa	K3	2921 ± 31	
		RTT-3803.3–8	3803.3–8 (3803.5 is separated in Sharon et al. 2007)	K4	2870 ± 82	
		LSC-3802.1	3802.1	K5	2870 ± 35	
		RTT-3802.3–5	3802.3–5	K6	2842 ± 29	
		LSC-3803.1	3803.1	K7	2893 ± 35	
	Seeds		3796	K8	2855 ± 29	
		Charcoal	3801	K9	2674 ± 30	
	Tell Qasile X (for context see text)	Seeds	T-18161a, aa	3932a, aa	QS1	2818 ± 26
			RTT-3932.3–6	3932.3–6	QS2	2692 ± 24 ^e
RTT-3931.3–5			3931.3–5	QS3	2911 ± 26	
LSC-3931.1			3931.1	QS4	2853 ± 25	
			GrN-27719 ^f	QS5	2895 ± 25	
RTT and T			3853.1,3,4	QS6	2753 ± 22	
T			3930	QS7	2800 ± 25	

Table 2 The end of Iron Age I. (Continued)

Site	Sample	Lab # (Boaretto et al. 2005 or Boaretto 2006)	Sample # (Sharon et al. 2007)	Code # in present paper	¹⁴ C BP date or average of several dates ^a
		T	3933a, aa	QS8)	2882 ± 28
		GrA-25535	Same sample as 3931	QS9	2864 ± 40
		GrA-25710		QS10	2818 ± 38
		GrA-25768		QS11	2897 ± 44
Tel Dor	D2/9–10 Irl(I) Olive stones			4531	D1
			4532	D2	2783 ± 22
Tel Hadar IV	Grain from silo		3795.3	HD1	2791 ± 52
			4291 (8 replications)	HD2	2853 ± 13
Tell el-Hammah “Lower”	Charcoal		4416	HM1	2779 ± 23
	Seeds		4417	HM2	2790 ± 23
Tel Rehov D-3 Locus 2862	Olive stones	RTT-3805.3–5	3805	R3a	2800 ± 20 ^g
		GrA-19033		R3b	2835 ± 45
		GrN-26119			2720 ± 30

^aAverages are cited from Boaretto et al. (2005), Boaretto (2006) (from Megiddo), and from Sharon et al. (2007) (for samples not mentioned by Boaretto et al. 2005 and Boaretto 2006).

^bAverage of MG5 and MG6 in Sharon et al. (2007) is 2920 ± 25.

^cCited from Sharon et al. (2007) due to an additional reading published by Boaretto (2006).

^dSharon et al. (2007) combined average for Y3, Y4, Y11–12 is 2816 ± 11.

^eAn average of 4 dates. Two additional dates from sample 3932 were published in Sharon et al. (2005, 2007). The following is a list of the Tell Qasile RTT-3932 dates (after Sharon et al. 2005:86; see their discussion): RTT-3932.3: 2745 ± 45; RTT-3932.4: 2765 ± 75; RTT-3932.5: 2685 ± 50; RTT-3932.6: 2650 ± 40; RTT-3932a: 2780 ± 35; RTT-3932aa: 2862 ± 40. See further discussion below.

^fPreviously unpublished date measured at Groningen University. See Footnote 8.

^gThe average calculated by Mazar et al. (2005:211). See Boaretto et al. (2005:52, Table 3 and Footnote d).

Table 2a Charred beams from the destruction level of Megiddo VIA (K-4 in Tel Aviv University excavations).

Lab #	Code # in present paper ^a	BP date
RT-2700	MG17	2895 ± 25
RT-2701	MG18	2845 ± 45
RT-2702	MG19	2890 ± 25
RT-3216	MG20	2825 ± 25
RT-3217	MG21	2830 ± 20
RT-3218	MG22	2805 ± 25
RT-3219	MG23	2870 ± 20
RT-3220	MG24	2820 ± 40
RT-3221	MG25	2850 ± 20
RT-3222	MG26	2875 ± 20
RT-3223	MG27	2955 ± 20
RT-3224	MG28	2695 ± 20
RT-3225	MG29	2525 ± 20
RT-3226	MG30	2865 ± 55
RT-3227	MG31	2775 ± 25

^aMG17–19 after Carmi and Segal (2000:502, Table 19.1). MG20–31 after Boaretto (2006:554–555). Most samples are of olive tree wood. All dates in this table were measured at Rehovot by Israel Carmi using the decay counting technique (Boaretto 2006: 553). For calibrated dates, see Boaretto (2006:554).

Megiddo Stratum VIA (Tel Aviv University Level K-4). Seven short-lived samples from K-4 were published, providing 12 dates (Boaretto et al. 2005; Boaretto 2006:553–557; Sharon et al. 2007:29). One of the samples (3945 = MG7–8) is described as coming from the occupation layers earlier than the final destruction, and 6 come from the destruction layer itself. Based on these samples, Finkelstein and Piasezky (2006a:48, 2006b:383) calculated the end of K-4 (=VIA) to a wide range of years: 1015–920 BCE, which would fit all 3 chronological systems. It should be noted that in 3 cases of short-lived samples (3944, 3945, and 3946), the latest calibrated date in the 68% range is earlier than 1000 BCE (Sharon et al. 2007:42). Our calculation (below and Figure 3A) indicates a range between 1010–943 BCE for the destruction of Stratum VIA (68% range), a date that fits the HC and MCC, but not the LC.

Fifteen ¹⁴C dates of charred beams (mostly of olive wood) from Level K-4 (=Stratum VIA) found in the destruction at Megiddo were analyzed at Rehovot in the late 1990s (Table 2a, based on Boaretto 2006:554). They provided a variety of dates from the 12th to the 8th centuries BCE. MG20, 21, 22, and 24 may support all 3 methods; MG17, 23, 26, and 27 may support only the HC (though they may be interpreted as old wood); MG18, 19, and 25 may support both the HC as well as the MCC, and MG28 and 29 provide dates in the 9th and 8th centuries BCE that are too low for any of the chronological systems. Two solutions may be suggested in this case: either MG28 and 29 are outliers, or the entire batch is biased towards lower dates.⁴

Based on the ¹⁴C dates from Megiddo (which were cited before their detailed publication appeared), Finkelstein (2002:121) claimed that “recent radiocarbon samples from Megiddo [K-4] all point to a 10th century date of this phase in the history of northern Israel.” More recently, Finkelstein et al. (2006:850) claimed that “the series of ¹⁴C results from Level K-4 (from both timber and short-lived samples) have not resolved the dispute, though according to Finkelstein and Piasezky, they seem to fit the Low Chronology system better.” This is hardly the case. The dates of the short-lived samples from Megiddo K-4 cannot support the Low Chronology, while the dates of the timbers are questionable and should not be taken into account in an evaluation of the date of Stratum VIA (see Footnote 4).

Yoque‘am Stratum XVII. In terms of material culture, Yoque‘am XVII corresponds to Megiddo VIA. Three short-lived samples (17 dates including replications) are published, with poor agreement between some of them (see discussion below). The calibrated averages of the 3 dates in the 68% probability range were calculated by Sharon et al. (2007:43) as being between 1120–995 BCE; we calculated 1045–997 BCE (Figure 3B; note, however, the reservations concerning the statistical validity of these dates, below). These dates fit the HC and MCC, but negate the LC.

Tell Keisan Stratum 9a. Three charcoal samples and 1 sample of seeds were measured. All except K9 fit the HC or MCC; none fit the LC. It thus appears that K9 is an outlier. A suspicion of the old-wood effect may be valid in the charcoal examples; thus, they are excluded from some of our models. The single short-lived sample (3796) is calibrated to 1060–930 BCE and thus could fit the HC and MCC, but not the LC.

⁴The dates in Table 2a were measured during the late 1990s by the decay counting method at Weizmann Institute Laboratory. As discussed elsewhere, several measurements made during the same years in the same laboratory on samples from Tel Rehov proved to be later by more than 100 yr than similar samples measured more recently at both Groningen and Rehovot/Tucson by AMS and LSC (Mazar 2004:32; Mazar et al. 2005: passim). This should be taken into account when considering the low dates of some of the timber samples from Megiddo K-4 (=VIA), which contradict the dates achieved now by the Iron Age Dating Project on short-lived samples from the same level.

Tell Qasile Stratum X. The severe destruction layer at Tell Qasile Stratum X yielded several concentrations of seeds found in bins. Twenty radiometric dates including replications are available from 7 samples (Boaretto et al. 2005; Sharon et al. 2005, 2007); QS5 is a new date added here.⁵ Samples 3931 and 3932 and GrN-27719 (QS1–5 and QS 9–11) are of *lathyrus* seeds found in a small bin in Room 168 of Stratum X. Sample 3853 (QS6) is a sample of charred grain found in the small bin C653, which was also attributed to Stratum X (Mazar and Harpazi-Ofer 1994). Sample 3933 (QS8) is of seeds found on the floor of Temple 131 of Stratum X (Mazar 1980). QS1 (part of sample 3932, average of 2 dates) fits the HC or MCC, while QS2 (another part of sample 3932, an average of 4 dates) should be defined, in our opinion, as an outlier, since the 9th century BCE calibrated date is improbable in light of archaeological considerations and in light of the other dates from Tell Qasile (see below).⁶ QS3 (part of sample 3931, average of 3 dates) is too high for both chronological systems, while QS4 (another date from sample 3931) fits the HC or the MCC system, but negates the LC. Samples QS9–11 (measured at Groningen) fit the HC.

Figures 3C1 and 3C2 show the combined dates from Tell Qasile with and without the outlier QS2. Figure 3C2 indicates a date that may fit only the HC and is somewhat too high even for the MCC. In any case, the LC is excluded.

Tel Dor Phases 9–10 in Area D2. These phases were attributed by the excavators to the late Iron Age I (Gilboa and Sharon 2003). The calibrated dates of the averages of samples 4531 and 4532 (D1–D2) are in the 10th century BCE. The upper ends of the 68% range of both may fit the MCC, while the lowest end may fit the LC. The 95% range enables all 3 chronological systems.

Tel Hadar Stratum IV. This is a prime context for the end of the Iron Age I, since it produced large amounts of grain from a granary. The imported Phoenician Bichrome vessels and a Greek (Euboean) Proto Geometric *lebes* add much to the importance of this site for Phoenician and Greek chronology. The average calibrated dates of this context (referring only to the dates published by Sharon et al. 2007) are 1043–979 BCE in the 68% probability range, which can fit the HC or MCC and negate the LC.

Tell el-Hammah “Lower”. This level is known only from a small probe (Cahill 2006) and the amount of published pottery is too small to define its nature. It could fit either the end of Iron I or the early part of Iron IIA, and thus we exclude it from our discussion of the end of Iron Age I.

Tel Rehov Stratum D-3. This phase includes a series of pits found in 2 excavation squares in Area D. They contained a small amount of pottery that may be attributed to the very end of the Iron Age I (Mazar et al. 2005:208–212).⁷ The single date R3a covers the entire 10th century and thus could fit all 3 systems. Sharon et al. (2007) added to it GrA-16757, but this is a mistake; the 2 Groningen dates from the same locus are GrA-19033 and GrN-26119 (published in Mazar et al. 2005). We added these 2 dates in Table 2 as our R3b. Note that the date of R8 in Table 3 was attributed by Sharon et al. (2007:31) to Stratum D-3 (their sample 3806), yet this sample came from Locus 1823

⁵Our thanks to Hendrik Bruins and Johannes van der Plicht for measuring this sample at the Groningen laboratories.

⁶Sharon et al. (2007:8–9) discuss the problem of sample 3932 and decided to eliminate the highest date in this set as an outlier. It seems more likely that the lowest one should be eliminated. In order to prevent bias, we have removed both QS1 and QS2 from some models (see below). Note that the averages in Sharon et al. (2007: Table 7) differ from the average in their Table 8.

⁷Note that a single date from D-3 measured during the late 1990s at the Weizmann Institute (RT-3120 from Locus 1858, 2670 ± 40; Mazar et al. 2005:198, 212) is much too low (see Mazar 2003:32). Its inclusion by Finkelstein and Piasezky (2003:774) may have caused the erroneous results reached in that study. Recent seasons at Tel Rehov have shown that the pits in Area D are a local phenomenon. Elsewhere, the last phase of Iron I includes substantial buildings.

of local Stratum D-2, which should be attributed to the earliest Iron IIA horizon (general Stratum VI). Five additional samples from the Stratum D-3 pits measured at Groningen yielded dates in the second half of the 11th and first half of the 10th centuries BCE (Bruins et al. 2005a:285, 2007:85–90; Mazar et al. 2005:197, 208–212).

Conclusion. The contexts described in this section are of the utmost importance for dating the end of the Iron Age I. As we have seen, most of the dates support the HC or MCC, and only a few may support the LC in addition to the HC/MCC.

IRON IIA CONTEXTS (TABLE 3)

Some 36 samples from 12 Iron IIA contexts, including 102 dates and replications, are presented in Table 3 (cited from Boaretto et al. 2005; Boaretto 2006:555; Sharon et al. 2007 and several additional sources). The following is a short analysis of some of these dates and their contexts.

Table 3 Span of the Iron Age IIA.

Site	Sample	Sample # (Boaretto et al. 2005)	Sample # (Sharon et al. 2007)	Code # in present paper	¹⁴ C BP date or average of several dates ^a
Tel Rehov D-2 Area D (=general Stratum VI)	Olive stones	RTT-3807.3–5	3807.3–5	R4	2757 ± 20 ^b
	Pit 1802	LSC-3807.1	3807.1a, 1b	R5	2770 ± 23
		GrN-26112		R5a	2805 ± 15
Tel Rehov E-1b Area E (=general Stratum V)	Olive stones	T-18159a, aa	3808a, aa	R6	2685 ± 25
	Locus 2618	RTT-3808.3–5	3808.3–5	R7	2678 ± 20
Tel Rehov D-2 Area D (=general Stratum VI)	Olive stones Locus 1823		3806	R8	2754 ± 24
Aphek X-8	Seeds	RTT-4511.3–5	4511.3–5	A1	2667 ± 20
Tel Dor D2/8c (Ir I/II)	Olive stones		4540 (3 repli- cations and 3 at Groningen)	D3	2757 ± 18
			4541.3–5	D4	2764 ± 22
			4542.3–5	D5	2779 ± 24
Tel Dor D2/8b (Ir IIa)	Olive stones		4556.3–5	D6	2750 ± 23
Megiddo H-5 (=IVB–VA)	Olive stones Locus 98/H/62/LB18	T-18167a, aa	3949a	MG13	2783 ± 32
		3949.3,4	3949aa	MG14	2859 ± 34
	Olive stones Locus 98/H/62/LB18	RTT-3948 ^c	—	MG15	2695 ± 50
	Cedar wood Locus 89/H/62	RT-3228 ^c	—	MG16	2770 ± 80
Yozne'am XIVb	Charcoal Locus 1734	RTT-3780.3–5	3780.3–5	Y8	2649 ± 31
		LSC-3780.1	3780.1, 1a	Y9	2725 ± 25 (for 3780.1 alone)
		T-18151a, aa	3780a, aa	Y10	2739 ± 35 (Boaretto et al. 2005; Sharon et al. 2007 av- erage of Y8–Y10: 2711 ± 11)
Horbat Rosh Zayit IIa	Seeds	LSC-3798.1	3798.1	RZ1	2745 ± 30
		RTT-3798.3–5	3798.3–5	RZ2	2755 ± 22

Table 3 Span of the Iron Age IIA. (Continued)

Site	Sample	Sample # (Boaretto et al. 2005)	Sample # (Sharon et al. 2007)	Code # in present paper	¹⁴ C BP date or average of several dates ^a
		T-18155a, aa	3798a, aa	RZ6	2689 ± 28 (Sharon et al. 2007 average date for RZ1,2,6: 2733 ± 15)
		LSC-3799.1	3799.1	RZ3	2745 ± 30
		RTT-3799.3	3799.3	RZ4	2729 ± 37
		T-18156a, aa	3799a, aa	RZ5	2692 ± 31 (Sharon et al. 2007 average date for RZ3– 5: 2722 ± 19)
			3797 (9 RTT replications)	RZ7	2709 ± 15
Bethsaida VI	Seeds	LSC-4281.1	4281.1a,b	BD1	2820 ± 35
		RTT-4281.3–5	4281.3–5	BD2	2786 ± 25 (Sharon et al. 2007 average date for BD1– 2: 2815 ± 17)
Hazor XB	Olive stones Locus 8595	T-18154a, aa	3786a, aa	HZ11	2639 ± 31 ^d
		RTT-3786.3–5	3786.3–5	HZ12	2585 ± 126 ^d (Sharon et al. 2007 average date for HZ 11–12: 2650 ± 25)
Hazor XA	Charcoal Locus 8034	T-18152a, aa	3783a, aa	HZ13	2700 ± 27
		RTT-3783.3–5	3783.3–5	HZ14	2777 ± 24 (Sharon et al. 2007 average date for HZ13–14: 2720 ± 20)
			3782.3–5	HZ17	2645 ± 31 ^d
Hazor IXA	Olive pits	RTT-3784.3–6	3784.3–6	HZ18	2632 ± 27 ^d
	Olive stones	T-18153a, aa	3785a, aa	HZ15	2697 ± 24
		RTT-3785.4–6	3785.4–6	HZ16	2689 ± 27 (Sharon et al. 2007 average date for HZ15–16: 2692 ± 21)
Tell el-Hammah “mid” level	Seeds		4411	HM3	2815 ± 29
			4420	HM4	2675 ± 23
	Semolina		4423	HM5	2688 ± 25
			4424	HM6	2687 ± 20
			4425	HM7	2701 ± 22
	Seeds		4412	HM8	2609 ± 21
			4413	HM9	2587 ± 23
			4414	HM10	2634 ± 23
			4415	HM11	2636 ± 23
			4418	HM12	2722 ± 24
			4419	HM13	2728 ± 28
Tell es-Safi temporary 4	Seeds		4409	SF1	2661 ± 30
			4410	SF2	2723 ± 18
Kadesh Barnea Stratum 4 (lowest fortress) ^e	Charcoal	GrN-12330		NH1	2930 ± 30
Nahal 'Elah ^e	Charcoal	GrN-15552		NH2	2840 ± 15

^aAverages are cited from Boaretto et al. (2005), Boaretto (2006) (from Megiddo), and from Sharon et al. (2007) (for samples not mentioned by Boaretto et al. 2005 and Boaretto 2006).

^bUnclear in Boaretto et al. (2005) if this is the average of 3 dates or just a single measurement of 3807.5. Sharon et al. (2007) gives an average of 2784 ± 11 for all 6 dates of sample 3807, including GrN-26112 measured at Groningen.

^cPublished by Boaretto (2006:555). Lacking in Sharon et al. (2007).

^dSee text for the problems involving these dates.

^ePublished in Bruins and van der Plicht (2005).

Tel Rehov IV–V. The measurements done by the Early Iron Age Dating Project fit the many dates of short-lived samples from Iron IIA strata at Tel Rehov measured at Groningen (Mazar et al. 2005: 200–201, 212–254). The dates of sample 3807 (R4 and R5) from Locus 1802 of Stratum D-2 (correlates with general Stratum VI) are similar to 3 dates from the same stratum (one of them from the same locus) measured at Groningen (GrN-26113, GrA-19030, GrN-26112). Sample 3808 (#R6–R7) from Stratum E-1b is somewhat low for this phase in Area E, which was considered as being parallel to general Stratum V. Yet, these samples came from accumulations of floor surfaces and debris in an open piazza (deeper than the uppermost surface in this courtyard), and thus the exact attribution of each individual layer to either general Stratum IV or V at Tel Rehov is not secure. A Groningen date (GrA-17260) from the same locus provides a somewhat higher date for this locus.

Tel Dor Phases 8c and 8b in Area D2. Phase 8c was defined by Gilboa and Sharon as belonging to a transitional IrI/IrII phase. In the view of one of us (Mazar), the published pottery (Gilboa and Sharon 2003:21–22, Figures 10–11) and the lack of similar “transitional” phases at other sites enables us to correlate this phase at Dor with Tel Rehov Stratum VI, namely with the early phase of Iron IIA (for this definition, see Herzog and Singer-Avitz 2006). The dates of sample 4540 may fit the LC in the 68% range and both the MCC and LC in the 95% range, while samples 4541 (970–840 BCE) and 4542 (975–895 BCE) fit both the MCC and LC in the 68% range. Sample 4556 (920–840 BCE), from the later phase 8b, fits both the MCC and LC.

Megiddo Level H5 (=IVB–VA). This stratum stands at the heart of the chronological debate: it was identified by Yadin and others as the Solomonic 10th century city, while Finkelstein suggested to lower its date to the Omride Dynasty in the 9th century. Sample 3949 (MG13 and MG14) clearly supports a 10th century BCE date (its average calibrated date is 1000–930 BCE; Sharon et al. 2007: 43), while sample 3948 (MG15) (Boaretto 2006:555; not mentioned by Sharon et al. 2007) supports a 9th century date. Sample 3228 (MG16; Boaretto 2006:555; not mentioned by Sharon et al. 2007) could fit both systems, but since this is a date of a cedar tree it is excluded from our models. Note that no dates are available from Stratum Vb.

Yoqne‘am Stratum XIV. The excavators defined 2 poor stratigraphic phases (strata XVI–XV) attributed to the early part of the Iron IIA following the violent destruction of Stratum XVII at the end of Iron Age I (Ben-Tor et al. 2005). These were followed by the rebuilding of a planned, fortified Iron IIA city (Stratum XIV), which was dated by the excavators on the basis of the HC to the second half of the 10th century BCE. The charcoal sample 3780 (numbers Y8–10) provides a range of dates with considerable differences. The average calibrated average is 895–815 BCE (Sharon et al. 2007:44). Note that Y8 is too low for all the chronological systems in the 68% probability range. These dates may indicate that the fortified city at Yoqne‘am was destroyed during the 9th century, though the city might have been constructed earlier.

Horbat Rosh-Zayit Stratum IIa. Three strata were attributed to the Iron Age IIA: Stratum III is a village site and strata IIb and IIa are 2 phases of a fortified citadel (Gal and Alexandre 2000). The 2 seed samples came from the *last* phase of this citadel (Stratum IIa) and thus determine the end of the Iron IIA fortress. The average calibrated dates of the 3 samples 3797–3799 is consistent between 900/895 and 840/820 BCE. These results may fit the excavators’ date for the destruction of Stratum IIa in the first quarter of the 9th century BCE. They fit both the MCC and the LC. Considering that there are 2 earlier Iron IIA strata from which no ¹⁴C dates are available, the long duration of the Iron IIA as suggested by the MCC, starting somewhat during the first half at the 10th century, may be supported. The material culture at Rosh Zayit very much resembles that of Tel Rehov strata V and IV.

Hazor Strata X–IX. Five samples from Ben-Tor’s excavations at Hazor represent strata X and IX. Stratum Xb was dated by Yadin and Ben-Tor to the Solomonic era in the 10th century, Stratum Xa to the post-Solomonic era at the end of the 10th century, and Stratum IXb-a to pre-Omrude early 9th century BCE. The dates of sample 3786 (HZ11–12) from Stratum Xb (calibrated age 825–795 BCE) are too low according to all the chronological systems. Since these dates are even lower than those of strata Xa and IXa, which are stratigraphically later, we suggest that this sample is an outlier; there might have been a problem such as contamination by a later intrusion, a mistake in the stratigraphic attribution, a mistake in registration, etc. Three samples are available from Stratum Xa. One is a charcoal sample (3783 = HZ13–14) that may fit all 3 chronological systems (its upper calibrated date is 895 BCE in the 68% range and 910 in the 95% range). Sample 3782 (H17, calibrated 905–840 BCE in 68% range) could fit at the upper end of the calibrated date Yadin’s date for this stratum, but could also fit the LC. Sample 3784 (calibrated date 815–790 BCE) is too low for all the chronological systems and is suspected to be an outlier like 3786.⁸ Sample 3785 (=HZ15–16) from Stratum IXa (calibrated average 890–805 BCE) can fit all 3 chronological systems. As seen, 2 of the Hazor dates—3786 (HZ11–12) and 3784 (HZ18)—are too low and should be regarded as outliers or mistakes made during the excavation; thus, they were not included in our Bayesian models.⁹

Bethsaida. Sample 4281 (BD1–2) is of charred grain found in a granary of Stratum VI below the monumental gate structure of the Iron II city, and attributed by the excavator R. Arav to the Iron Age IIA. Since published pottery is not yet available, it is difficult to assess this definition, though description of red slipped and burnished pottery from this level strengthens the attribution to Iron IIA. The calibrated date of 1000–930 BCE (Sharon et al. 2007:43) may fit the HC or MCC, but negates the LC.

Tell el-Hammah. This site in the Jordan Valley, south of Tel Rehov, was excavated on a small scale. The lower level provided calibrated dates between 975–905 BCE, and since this level was attributed by Cahill (2006) to the late Iron I, this date seems to support the LC. Yet, the small amount of published pottery (Cahill 2006:436) is insufficient to say whether this phase should be correlated with Tel Rehov Stratum D-4/D-3 (late Iron I) or with Tel Rehov Stratum VI (early Iron IIA). The latter possibility would support the HC or MCC. The “middle” stratum pottery from Tell el-Hammah is identical to Rehov strata V–IV. The 11 dates from this phase are scattered from 2815 to 2587 BP; thus, their reliability may be questioned. One sample (4411) provided a calibrated date in the 10th century, while 5 samples provided dates at the end of the 9th and early 8th centuries and the other 5 cover most of the 9th century. The latter may fit both the MCC and LC, yet the deviations in the other samples remain unexplained.

Tell es-Safi. The 2 dates of samples from Temporary Level 4, 4409 and 4410 (SF1–2), are calibrated to 835–795 and 895–835 BCE. They come from the rich destruction level attributed to Hazael, King of Damascus, about 830–810 BCE (Maier and Ehrlich 2001). This historical date fits the lowest edge of the 68% probability range of SF2 and the upper edge of SF1.

Negev Highland. Two dates from Iron IIA contexts in the Negev Highlands are available: NH1 and NH2 (Bruins and van der Plicht 2005). The most acceptable archaeological date for these sites is the 10th century BCE. Both samples are of charcoal and thus could be of old wood. NH1 is indeed much too old, while NH2 fits a 10th century date.

⁸Sharon et al. (2007) present 2 contradictory averages for sample 3782. We use here the average 2645 ± 31 (Sharon et al. 2007:35) rather than 2741 ± 18 (Sharon et al. 2007:43), which must be a mistake.

⁹Several unpublished samples from Hazor measured at Groningen indicate dates that agree in most cases with the conventional chronology. We thank A Ben-Tor and S Zuckerman for showing us the results.

Conclusion. The many and varied dates from Iron IIA contexts cover both the 10th and 9th centuries BCE, in accord with the MCC. Many are in the 9th century BCE, as they come from destruction layers from the end of the period. Yet, the long duration of the period is emphasized by the dates of the last Iron I contexts as described in the previous section and by the existence of earlier Iron IIA levels, not represented in the ^{14}C record. The division of the Iron Age IIA into 2 sub-periods—early and late—as suggested by Herzog and Avitz-Singer (2006; see also Sharon et al. 2007:10–13 and our comment above in relation to Tel Dor) is now substantiated in the excavations of Tel Rehov, where Stratum VI represents the earlier phase of the period and strata V–IV the later phase. The date of transition between these 2 sub-periods is one of the questions to be resolved in future research.

ALTERNATIVE BAYESIAN MODELS AND STATISTICAL CALCULATIONS

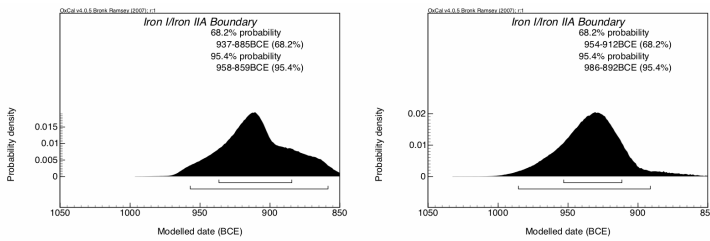
In the following section, 4 Bayesian models are presented with some variations (Figure 1). The OxCal specifications for each model are given in the Appendix (available with the online version of this article at <http://radiocarbon.library.arizona.edu/>).

Model A

We first tried to reproduce the results of the analysis performed by Boaretto et al. (2005). This involved the analysis of results from samples listed in their Tables 1–3. We included the dates measured at Arizona and those measured at the Weizmann Institute of Science Radiocarbon Laboratory (Rehovot) both by AMS (RTT) and liquid scintillation (LSC) and those measured by the Groningen lab on the same material and mentioned in their paper.¹⁰ We have not included in Model A the 2 dates BD1–2 from Bethsaida, since these are not definitely attributed to Iron I or Iron II by Boaretto et al. (2005), though we are confident that their context is Iron IIA (see above and below). Rather than averaging all of the individual measurements, we used the averages given in their table for measurements made at 1 laboratory by 1 method. We then combined all of the samples for 1 context since these are assumed to be the same age. This reproduced fairly well their analysis termed “Combined with Outliers, Rehovot and Tucson” shown in their Table 4, as shown in our Figure 1A1.

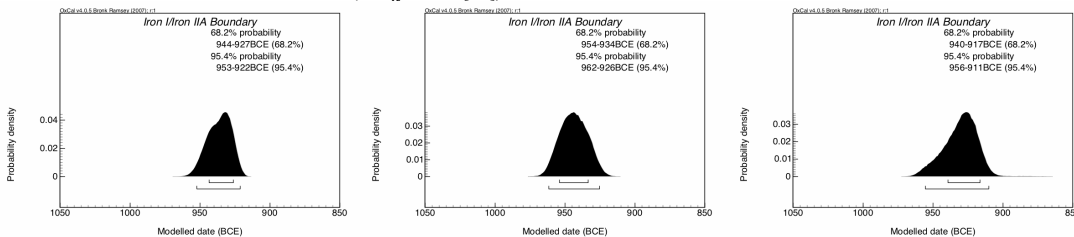
However, we cannot see the justification for the next stage of their analysis. They identify QS1 (T-18161 = 3932a, aa) from Tell Qasile X as an outlier. Yet, while both Tucson dates for QS1 (T-18161aa and T-18161a) agree with each other and the Rehovot/Tucson results for this sample (QS2 = RTT-3932.3–6) are also internally consistent, there is a very marked disagreement between the 2 labs on this 1 sample (the χ^2 test gives $t = 12.7$ compared to the 5% threshold of 3.8). This sample from Tell Qasile is critical to the model (as recognized and discussed by Sharon et al. [2005:86–89, 2007:8–9]) and there is clearly something wrong here. In making any choice between QS1 (=3932a, aa) and QS2 (=3932.3–6), we would prefer the former (higher date) since it is supported by most of the other dates from Tell Qasile (Table 2). There is clearly some unexplained problem with this sample, and it seems more likely that QS2 is an outlier rather than QS1. In order not to let this result bias the model in either direction, we remove both QS1 and QS2 and get a markedly different solution (see our Figure 1A2). We realize that other dates from Qasile are of essentially the same material, but the discrepancy evident in the first dates does not seem to be reproduced to the same extent in other dates. This also leaves a model with a good agreement index. Three other samples (HZ14 from Hazor Xa, Y6–Y7 [RTT-3779] from Yoqne‘am XVII, and R1 from Tel Rehov D-3) have marginally high χ^2 values.

¹⁰As said above, only the 5 dates measured at Groningen and cited in Boaretto et al. (2005: Table 3) were included in our model, as we assume that they were included in their model as well.



A1
Averaged dates from Tables 1, 2, and 3 of Boaretto et al. (2005). Average dates are combined before calibration.

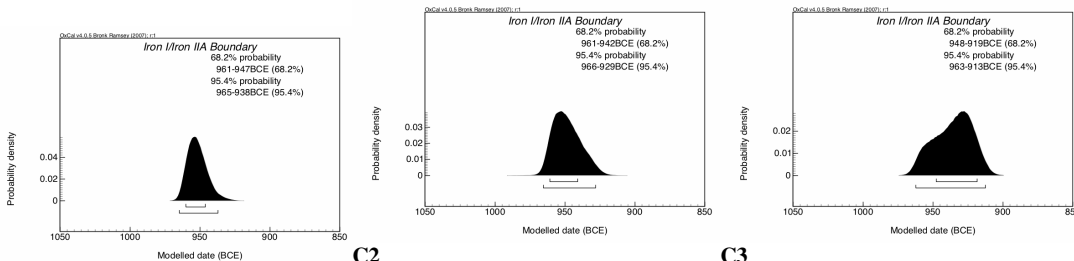
A2
Removed: QS1 & 2 (fails $\chi^2 T = 12.7$ [3.8]) – this results in all agreement indices passing; Left in: HZ13-14 (fails $\chi^2 T = 4.5$ [3.8]) and Y6-7 (fails $\chi^2 T = 5.8$ [3.8]).



B1
Other relevant published dates; excluded BM3 & 4; HZ11, 12, 17 & 18; MG28 & 29; HM1 & 2 as discussed in text.

B2
Removed outliers: QS1, 2 & 6; NH1; HZ3, 4, 5, 8, 9 & 10; HV1 & 2; K9. Overall model agreement then ok at 83.9%.

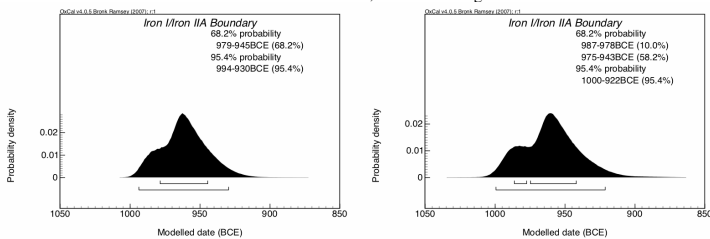
B3
Removed all charcoal and wood and reinstated QS6.



C1
Three-phase model with same data as in B1.

C2
Removed outliers: QS1 & 2; NH1; HZ4, 5, 9 & 10; K9. Overall agreement then ok at 70.4%.

C3
As C2 but also removed all charcoal and wood.



D1
Multi-phase model for Megiddo using charred beams as a TPQ for the Iron I/Iron IIA transition. MG28 and MG29 rejected on visual inspection. Overall model agreement is 64.4%.

D2
Multi-phase model for Megiddo – only short-lived material used. No dates rejected; agreement is slightly low on MG9, MG10, and MG15; overall model agreement is 43.7%.

Figure 1 Bayesian models A–D

Model B: Two Phases, with Other Additional Data

Model B includes additional published dates relevant to the analysis (see Tables 2–3; dates HZ11, 12, 17, and 18; MG28 and 29; HM1 and 2 are not included for reasons discussed above).

The results of this analysis are shown in Figure 1B1. However, the overall model agreement is poor (12.6%). In particular, looking at the dates in detail, it can be seen that the date for samples QS1 (RTT-3932 from Tell Qasile X, late Iron I) is later even than dates of Iron IIA samples like MG14 from Megiddo IVB–VA and BD1–BD2 from Bethsaida VI (Table 3). It would be possible to remove the dates MG14 (=RTT-3949) and BD1–BD2 (=RTT-4281), but both are dates of olive stones and seeds, respectively, and there is no reason to suppose they are wrong. From the argument above, we feel that removal of QS1 and QS2 (RTT3932) is more logical given the poor internal agreement (see discussion above). NH1 (charcoal sample) is also clearly too early to be consistent with other dates (agreement <1%). We also removed early charcoal dates from Hazor XII/XI (HZ4, HZ5, HZ9, and HZ10 explained above as samples of old wood in secondary use) and HZ3 and HZ8 as they have a poor agreement index, being considerably earlier than the rest of the now much larger group of dates for Iron I and therefore incompatible for a simple model with 2 uniform phases. We also removed from this model HB1 and HB2 since they are of charcoal, though they could fit an Iron I date. The other samples with low agreement indices that we removed from the analysis are K9 (agreement 0.1%) and QS6 (agreement 25.3%), which are much later than others in the Iron II group. We then get a date for the transition from Iron I to Iron II as shown in Figure 1B2. This model now includes all of the data that we think are needed in the model. Because, in principle, any charcoal or wood date might be significantly older than its context, even though it is not obviously an outlier, we also considered Model B3, the results for which are shown in Figure 1B3. In this model, we included only short-lived material. In other respects, this model is similar to B2 except that QS6 can still be retained in the analysis while retaining a good overall agreement.

Model C: Two Phases with an Overlapping Late Iron I Phase

We now tried to improve on the modeling of the phases. Because the material in Table 2 comes from contexts right at the end of Iron I, it seems sensible to treat these dates separately from the samples listed in Table 1 that might be considerably earlier. We also class the charcoal dates in Table 2a as being from Iron I, but possibly earlier than the destruction levels as they are dates of charcoal from beams. The only material in Table 2 that might be earlier are the 2 dates MG7 and MG8, which are defined as “pre-destruction.”

We constructed a 3-phase model on these lines. First, we had a simple 2-phase model for LBA/Iron I and Iron IIA. In the first of these phases, we had the dates from Tables 1 and 2a and the dates MG7 and MG8 from Megiddo VIA (pre-destruction). These dates might reasonably be supposed to come from any time in Iron I or the very end of the LBA. In the second phase, we put all of the dates from Table 3 that are Iron IIA. The transition between these 2 phases is labeled “Iron I/Iron IIA.” We now have a third independent phase, consisting of the short-lived material from the very end of Iron I given in Table 2. We constrain this phase to end at the same time as the “Iron I/Iron IIA” transition. We expect this phase to be much shorter than the LBA/Iron I phase. We do not constrain the dates within this to be later than the others though. A schematic depiction for this model is shown in Figure 2.

The results of this model are shown in Figure 1C1. Now we do not need to remove HZ3 and HZ8 or HB1 and HB2 as we did for Model B2, as the model allows for some earlier dates in the longer LBA/Iron I phase and perhaps because the model better reflects the data. We do still need to remove NH1, K9, QS1, QS2, HZ4, HZ5, HZ9, and HZ10 in order to get a good level of agreement (taking this from 19.8% to 70.4%), and this is done in Model C2. Finally, as for Model B, we looked at the sensitivity of the model to the presence of wood and charcoal: Model C3 is the same as Model C2, but eliminates all wood and charcoal dates. This eliminates all of the data from some contexts, so this model does not include so much chronological information; however, this model is free from any possible bias to older ages from old-wood effects.

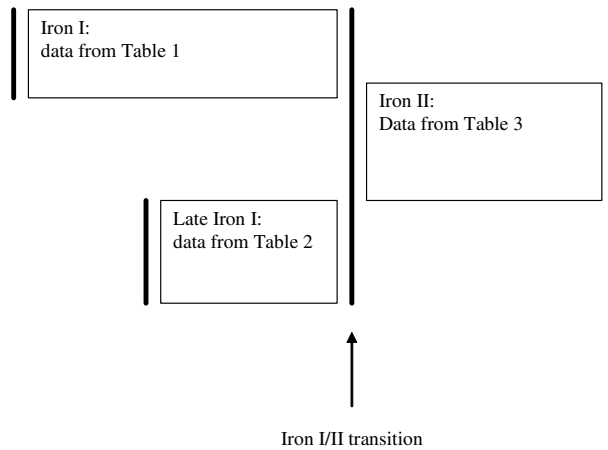


Figure 2 Schematic Bayesian Model C

Models B and C contain much more data in them and are less dependent on the removal of outliers (though this is necessary to get a self-consistent model). All models that we have looked at that use the broad phasing, except for Model A1, point to a date for the Iron I/II transition in the middle of the 10th century BCE. Model C2 would seem to us the most realistic, while retaining the maximum information with a date for the transition of 961–942 BCE (68.2%) or 966–929 BCE (95.4%). Model C3, with only short-lived material, is also important for comparison and gives an age range of 948–919 BCE (68.2%) or 963–913 BCE (95.4%).

Model D: Single Site

Finally, we come to another important issue with these models that needs to be addressed. The underlying assumption of the models is that there is a synchronous change from Iron I to Iron II across the region. Given the sensitivity of the models to single dates from 1 site, it could be that this is biasing the results in a significant way, if at 1 or 2 locations the transition in the type of material culture took place at a different time. To test this, we have looked at the dates only from Megiddo, since this has the greatest number of dates from this horizon of any of the sites investigated here. While discarding MG16 on the grounds that it could be old wood, we use a model for Megiddo with 5 main phases:

- Megiddo K-6 (=VIIA)
- Megiddo K-4 (=VIA) pre-destruction
- Megiddo K-4 (=VIA) destruction
- Megiddo K-3/H-6 (=VB) (no dates)
- Megiddo H-5 (=IVB–VA)

The Iron I/Iron II transition occurs between the K4 (=VIA) destruction and the level K3/H6 (=VB) where there are no dates. In addition, in Model D1 we included a sixth phase, which consisted of the dates of charred timber from Stratum K-4 (VIA) as detailed in Table 2a, excluding MG28 and MG29, which are clear outliers. This phase is constrained to end at the Iron I/II transition and has an exponential distribution of dates (rising to a maximum at the transition itself). This model is totally internally consistent. In Model D2, we removed the dates of the charred timber (Table 2a) from the

model and used a simple 4-phase model as discussed above. The results of these models are shown in Figure 1D2 and are entirely consistent with the overall picture obtained from the model that summarizes the region as a whole (in particular see Model C2). They suggest that the transition date from Iron I to Iron II at Megiddo occurred in the range 987–978 (10%), 975–943 (58.2%), or 1000–928 BCE (95.4%). In these models, we have included the phase K3/H6 (=VB) even though there are no dates associated with it, because it clearly represents some time in the development of the site; if this phase is omitted, the dates for the Iron I/II transition move about 10 yr later.

Dating Destruction Layers from the End of the Iron Age I

Finally, to reduce some of the data to their simplest level, we tested the assumption that the samples from specific destruction layers (Megiddo VIA, Yoqne‘am XVII, Tell Qasile X, and Tel Hadar IV) reflect a single event. This does not require Bayesian analysis at all. All we had to do is to combine the dates before calibration and perform a χ^2 test to test the hypothesis that they are contemporary. In 3 of the cases (Megiddo K-4, Yoqne‘am XVII, and Tell Qasile X), the results do not pass this test: see Figure 3A–C. In the case of Tell Qasile X, the agreement between the results is very poor and only if we reject the 2 earliest and the 2 latest dates (QS2, 3, 6, and 11) do the results pass the χ^2 test. However, these combinations do consistently suggest that a date as late as 920 BCE for these contexts is very unlikely.

The overall ranges from this simple analysis (rejecting QS2, 3, 6, and 11) are as follows:

End of Tell Qasile X: 1039–979 BCE (68.2%), 1051–938 BCE (95.4%).

End of Megiddo VIA: 1010–943 BCE (68.2%), 1040–927 BCE (95.4%).

End of Yoqne‘am XVII: 1013–944 BCE (68.2%), 1044–932 BCE (95.4%).

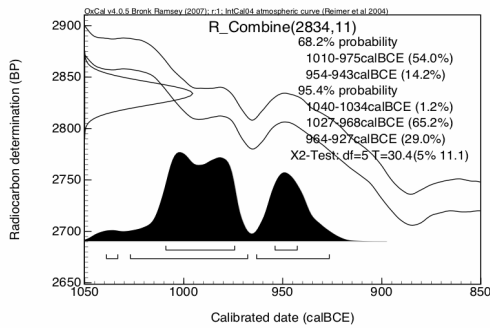
End of Tel Hadar IV: 1043–979 BCE (68.2%), 1054–932 BCE (95.4%).

All of these conclusions from combining dates that are clearly more scattered than they should be for a single event should be treated with considerable caution. However, it is very hard to see how these dates can be taken as evidence for the end of the Iron Age I at these sites occurring in the late 10th century BCE. Figure 4 shows the average dates of the destruction events at the 4 sites mentioned above against the results of Models C2 and C3.

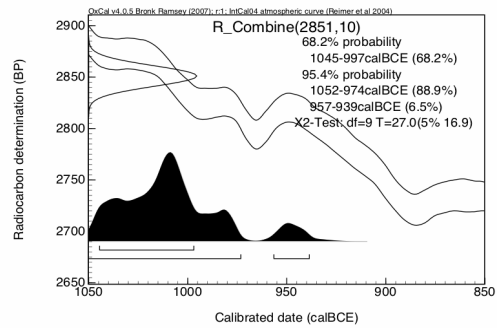
All of the generalized models presented here and in Sharon et al. (2007) assume a transition from Iron I/II, which is synchronous across the region. Our analysis of this transition, on essentially the same data sets, suggests that under such a model this transition took place in the middle of the 10th century BCE. Based on the above-mentioned dates of destruction layers assigned to the end of the Iron Age I and, given that we actually have very little datable material from the earliest phases of Iron II, this is likely to be a somewhat late estimate. More critically, however, if the transition from Iron I/II is a process that takes a generation, rather than an abrupt and synchronous event, then this process was almost certainly underway early in the 10th century BCE, even if it might not have been complete at all sites until the latter half of the 10th century BCE.

CONCLUSIONS

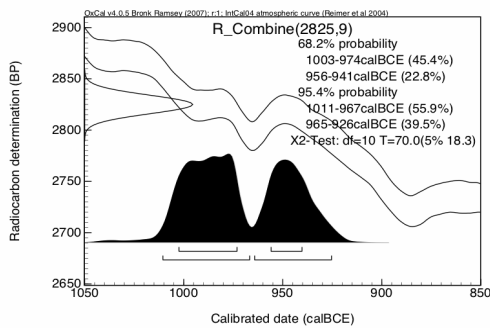
The conclusion presented by Gilboa and Sharon (2003), Boaretto et al. (2005), and Sharon et al. (Sharon et al. 2007:18–22)—that the transition from Iron I to Iron II occurred about 900 BCE—is questionable. In fact, Sharon et al. recently related to the entire second half of the 10th century BCE as a transitional period from the Iron I and Iron II.



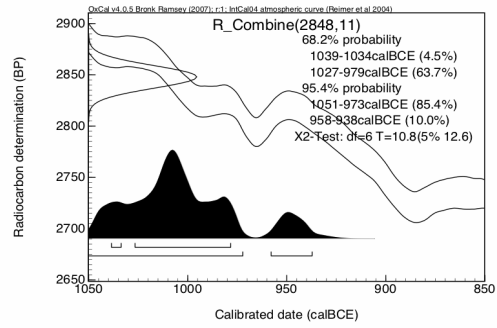
A
 Dates from Megiddo K-4 combined together – note the failed χ^2 test indicating that these results do not suggest a single age for all of the samples from the context.



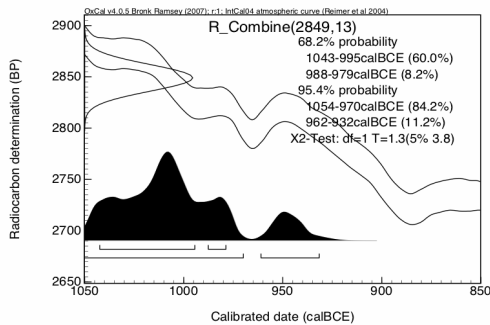
B
 Dates from Yoqneam XVII combined together; these results also fail a χ^2 test, though not quite as badly as those for Megiddo K-4, indicating that they do not reflect a single event.



C1
 Dates QS1-11 from Tel Qasile X combined together; the internal agreement is very poor indeed in this case.



C2
 After removing the 2 oldest and 2 youngest dates (QS2, 3, 6 and 11), these results just pass the χ^2 test for contemporaneity.



D
 Dates from Tel Hadar IV.

Figure 3A–D Combinations of dates from single destruction layers marking the end of Iron Age I.

In the survey of sites in the first part of this paper, we have seen that several key sites often mentioned in the chronological debate yielded dates that definitely contradict the LC. These include, among others, the short-lived samples from Megiddo VIA and IVB–VA, Tell Qasile X, and Tel

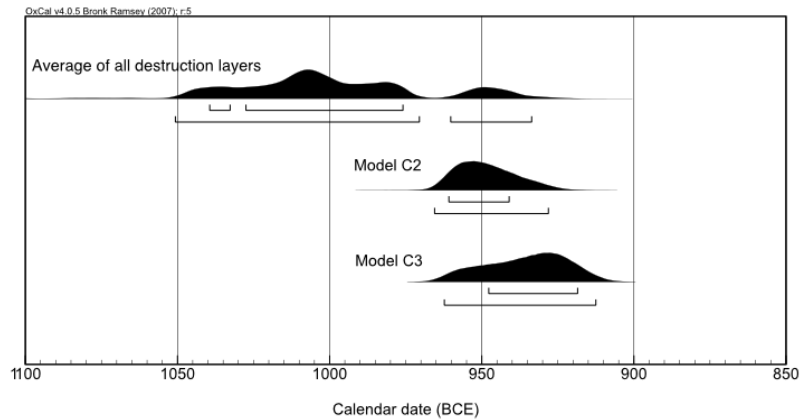


Figure 4 Comparison between the average of the destruction layers and Models C2 and C3 (shown in Figure 1).

Hadar IV (the latter has direct implications on Aegean chronology). Relating to other sites, we pointed out certain problems such as the contradiction between certain ^{14}C dates and the Iron II stratigraphic sequence at Hazor.

Our Bayesian models presented in the second part of the paper are based on the same data and use the same method as Boaretto et al. (2005), yet using additional dates (mainly from Sharon et al. 2007) and removing outliers to the extent needed to achieve good internal consistency.¹¹ This led to Model C2, which indicates a 68% probability date range of 960–940 BCE for the transition from Iron I to Iron II, while Model C3 would lower this date to 948–919 BCE. Model D2, based on short-lived samples from Megiddo alone, confirms the Model C2 results. The destruction dates of rich late Iron I contexts such as Tell Qasile X, Megiddo VIA, Yoqne‘am XVII, and Tel Hadar IV, all in a range between the last decades of the 11th and the mid-10th centuries BCE, support either Model C2 or even an earlier date in the 10th century for the end of Iron I. This sounds like a minor difference of a mere ~50 yr compared to the results of Boaretto et al. (2005), and may not be fully resolvable by ^{14}C ; yet, these years are at the very heart of the chronological and historical debate concerning the 10th century BCE. According to our Model C2, and to a less extent Model C3, combined with the destruction dates of late Iron I sites (Figures 3 and 4), the second half of the 10th century should be included in the Iron IIA.

An additional issue should be mentioned: as discussed above, the Iron Age IIA can be divided into early and late phases (Herzog and Avitz-Singer 2006), a phenomenon confirmed at Tel Rehov. Since most of the Iron IIA samples came from contexts related to the later part of the period—while the early part is hardly represented in the samples—some gap may exist between the well-dated “end of Iron I” contexts (Table 2 and Figure 3) and the large number of samples from more advanced Iron IIA contexts (most of the dates in Table 3). This may explain the gap between the destruction dates at the end of the Iron Age I and the results of our Models C2 and C3 for the transition Iron I/II (see Figure 4). It might be that the Bayesian models are not sensitive enough to accommodate such a situation. In such a case, the beginning of Iron IIA might have started somewhat earlier than the date suggested by our Models C2 and C3. Such an earlier date may fit the transition date from Iron I to Iron II as calculated at Tel Rehov (992–961 BCE range, 68% probability; see Mazar et al. 2005; Bru-

¹¹ Yet, our models do include questionable dates like those from Hazor Stratum X (except the outliers HZ11–12, 18).

ins et al. 2005a:287, Figure 15.4) and the approximate date ~980 BCE for this transition as suggested by Mazar (2005).

A word of caution should be expressed: because of the limited precision of the calibrated ¹⁴C dates themselves, the Bayesian models are sensitive and tend to provide considerably different results when a certain date is added or deleted from the model. In our case, the single date QS2 from Tell Qasile could change the results considerably, especially when only the dates from Boaretto et al. (2005) are included in the analysis. Continued publication and future analysis of data by the Early Iron Age Dating Project and other studies, as well as a more comprehensive study that will include all the available dates from this period (including all the Tel Rehov dates), may change the picture presented here.

REFERENCES

- Ben-Ami D. 2001. The Iron Age I at Tel Hazor in light of the renewed excavations. *Israel Exploration Journal* 51:148–70.
- Ben-Tor A, Zarzecki-Peleg A, Cohen-Anidjar S. 2005. *Yoqne'am II, the Iron Age and the Persian Period* (Qedem Reports No. 6). Jerusalem: The Hebrew University. 421 p.
- Boaretto E. 2006. Radiocarbon dates. In: Finkelstein I, Ussishkin D, Halpern B. *Megiddo IV: The 1998–2002 Seasons*. Tel Aviv: Tel Aviv University. p 552–7.
- Boaretto E, Jull AJT, Gilboa A, Sharon I. 2005. Dating the Iron Age I/II transition in Israel: first intercomparison results. *Radiocarbon* 47(1):39–55.
- Bruins HJ, van der Plicht J. 2005. Desert settlement through the Iron Age: radiocarbon dates from Sinai and the Negev Highlands. In: Levy T, Higham T, editors. *The Bible and Radiocarbon Dating: Archaeology, Text and Science*. London: Equinox. p 349–66.
- Bruins HJ, van der Plicht J, Mazar A, Bronk Ramsey C, Manning SW. 2005a. The Groningen radiocarbon series from Tel Rehov: OxCal Bayesian computations for the Iron IB–IIA boundary and Iron IIA destruction events. In: Levy T, Higham T, editors. *The Bible and Radiocarbon Dating: Archaeology, Text and Science*. London: Equinox. p 271–93.
- Bruins HJ, van der Plicht J, Ilan D, Werker E. 2005b. Iron Age ¹⁴C dates from Tel Dan: a High Chronology. In: Levy T, Higham T, editors. *The Bible and Radiocarbon Dating: Archaeology, Text and Science*. London: Equinox. p 323–36.
- Bruins HJ, Mazar A, van der Plicht J. 2007. The end of the 2nd millennium BCE and the transition from Iron I to Iron IIA: radiocarbon dates from Tel Rehov, Israel. In: Bietak M, Czerny E, editors. *The Synchronisation of Civilizations in the Eastern Mediterranean in the Second Millennium B.C. III*. Vienna: Verlag der Österreichischen Akademie der Wissenschaften. p 79–100.
- Cahill JM. 2006. The excavations at Tell el-Hammah: a prelude to Amihai Mazar's Beth-Shean Valley Regional Project. In: Maeir AM, de Miroschedji P, editors. *"I Will Speak the Riddles of Ancient Times," Archaeological and Historical Essays in Honor of Amihai Mazar on the Occasion of His Sixtieth Birthday*. Winona Lake: Eisenbrauns. p 429–60.
- Carmi I, Segal D. 2000. Radiocarbon dates. In: Finkelstein I, Ussishkin D, Halpern B. *Megiddo III: The 1992–1996 Seasons*. Tel Aviv: Tel Aviv University. p 502–3.
- Finkelstein I. 1993. Conclusions. In: Finkelstein I, Bunimovitz S, Lederman Z. *Shiloh, The Archaeology of a Biblical Site*. Tel Aviv: Tel Aviv University. p 371–93.
- Finkelstein I. 1996. The archaeology of the United Monarchy: an alternative view. *Levant* 28:177–87.
- Finkelstein I. 2002. The campaign of Shoshenq I to Palestine: a guide to the 10th century BCE polity. *Zeitschrift des Deutschen Palästina-Vereins* 118:109–35.
- Finkelstein I. 2005. A Low Chronology update: archaeology, history and the Bible. In: Levy T, Higham T, editors. *The Bible and Radiocarbon Dating: Archaeology, Text and Science*. London: Equinox. p 31–42.
- Finkelstein I, Piasezky E. 2003. Recent radiocarbon results and King Solomon. *Antiquity* 77(298):771–9.
- Finkelstein I, Piasezky E. 2005. ¹⁴C results from Megiddo, Tel Dor, Tel Rehov and Tel Hadar. In: Levy T, Higham T, editors. *The Bible and Radiocarbon Dating: Archaeology, Text and Science*. London: Equinox. p 294–301.
- Finkelstein I, Piasezky E. 2006a. The Iron Age I–IIA in the Highlands and beyond: ¹⁴C anchors, pottery phases and the Shoshenq I campaign. *Levant* 38:45–61.
- Finkelstein I, Piasezky E. 2006b. ¹⁴C and the Iron Age chronology debate: Rehov, Khirbet en-Nahas, Dan and Megiddo. *Radiocarbon* 48(3):373–86.
- Finkelstein I, Ussishkin D, Halpern B. 2006. *Megiddo IV: The 1998–2002 Seasons*. Tel Aviv: Tel Aviv University. 860 p.
- Gal A, Alexandre Y. 2000. *Horbat Rosh Zayit: An Iron Age Storage Fort and Village*. IAA Report No. 8. Jerusalem: Israel Antiquities Authority. 247 p.
- Gilboa A, Sharon I. 2001. Early Iron Age radiometric dates from Tel Dor: preliminary implications for Phoenicia and beyond. *Radiocarbon* 43(3):1343–52.
- Gilboa A, Sharon I. 2003. An archaeological contribu-

- tion to the Early Iron Age chronological debate: alternative chronologies for Phoenicia and their effects on the Levant, Cyprus and Greece. *Bulletin of the American Schools of Oriental Research* 332:7–80.
- Herzog Z, Singer-Avitz L. 2006. Sub-dividing the Iron Age IIA in northern Israel: a suggested solution to the chronological debate. *Tel Aviv* 33(2):163–92.
- Higham T, Najjar M, van der Plicht J, Bronk Ramsey C, Bruins HJ, Robinson M, Levy TE. 2005. Lowland Edom and the High and Low chronologies: Edomite state formation, the Bible and recent archaeological research. In: Levy T, Higham T, editors. *The Bible and Radiocarbon Dating: Archaeology, Text and Science*. London: Equinox. p 129–63.
- Levy T, Higham T, editors. 2005. *The Bible and Radiocarbon Dating: Archaeology, Text and Science*. London: Equinox. 448 p.
- Maeir AM, Ehrlich C. 2001. Excavating Philistine Gath: Have we found Goliath's hometown? *Biblical Archaeology Review* 27(6):22–31.
- Mazar A. 1980. *Excavations at Tell Qasile, Part One. The Philistine Sanctuary: Architecture and Cult Objects* (Qedem Reports No. 12). Jerusalem: The Hebrew University of Jerusalem. 153 p.
- Mazar A. 1990. *Archaeology of the Land of the Bible 10,000–586 BCE*. New York: Doubleday. 572 p.
- Mazar A. 2004. Greek and Levantine Iron Age chronology: a rejoinder. *Israel Exploration Journal* 54:24–36.
- Mazar A. 2005. The debate over the chronology of the Iron Age in the southern Levant: its history, the current situation and a suggested resolution. In: Levy T, Higham T, editors. *The Bible and Radiocarbon Dating: Archaeology, Text and Science*. London: Equinox. p 15–30.
- Mazar A, Carmi I. 2001. Radiocarbon dates from Iron Age strata at Tel Beth Shean and Tel Rehov. *Radiocarbon* 43(3):1333–42.
- Mazar A, Harpazi-Ofer S. 1994. The excavations at Tell Qasile from 1988 to 1991. *Israel – People and Land 1990–1993 (Eretz Israel Museum Year Book) 7–8:9–34*. In Hebrew.
- Mazar A, Bruins HJ, Panitz-Cohen N, van der Plicht J. 2005. Ladder of time at Tel Rehov: stratigraphy, archaeological context, pottery and radiocarbon dates. In: Levy T, Higham T, editors. *The Bible and Radiocarbon Dating: Archaeology, Text and Science*. London: Equinox. p 195–255.
- Sharon I, Gilboa A, Boaretto E, Jull T. 2005. The Early Iron Age Dating project: introduction, methodology, progress report and an update on the Tel Dor radiometric dates. In: Levy T, Higham T, editors. *The Bible and Radiocarbon Dating: Archaeology, Text and Science*. London: Equinox. p 65–94.
- Sharon I, Gilboa A, Jull T, Boaretto E. 2007. Report on the first stage of the Iron Age Dating Project in Israel: supporting the Low Chronology. *Radiocarbon* 49(1): 1–46.
- Stern E, editor. 1993. *The New Encyclopedia of Archaeological Excavations in the Holy Land*. New York: Simon and Schuster. 1552 p.
- van der Plicht J, Bruins H. 2005. Quality control of Groningen ¹⁴C results from Tel Rehov. In: Levy T, Higham T, editors. *The Bible and Radiocarbon Dating: Archaeology, Text and Science*. London: Equinox. p 256–70.

APPENDIX I – OXCAL SPECIFICATION FOR THE MAIN BAYESIAN MODELS

A1

```
Options()
{
  Resolution=1;
};
Plot()
{
  Sequence()
  {
    Boundary("Start");
    Phase("LBA/IAI")
    {
      Phase("Megiddo K-6")
      {
        Label("Olive stones");
        R_Combine("MG1-2")
        {
          R_Date("MG1", 2893, 27);
          R_Date("MG2", 2894, 23);
        };
        R_Combine("MG3-4")
        {
          R_Date("MG3", 2968, 30);
          R_Date("MG4", 2918, 22);
        };
      };
    };
    Phase("Tell Keisan 13")
    {
      Label("Charcoal");
      R_Combine("K1-2")
      {
        R_Date("K1", 2999, 29);
        R_Date("K2", 2984, 20);
      };
    };
  };
};
```

```
Phase("Hazor XII/XI")
{
  Label("Charcoal");
  R_Combine("HZ1 & 6")
  {
    R_Date("HZ1", 2945, 50);
    R_Date("HZ6", 2975, 35);
  };
  R_Combine("HZ2 & 7")
  {
    R_Date("HZ2", 2965, 50);
    R_Date("HZ7", 2940, 30);
  };
  R_Combine("HZ4 & 9")
  {
    R_Date("HZ4", 3650, 50);
    R_Date("HZ9", 3570, 53);
  };
  R_Combine("HZ5 & 10")
  {
    R_Date("HZ5", 3370, 60);
    R_Date("HZ10", 3375,30);
  };
  Label("Olive stones");
  R_Combine("HZ3 & 8")
  {
    R_Date("HZ3", 3060, 50);
    R_Date("HZ8", 3060, 30);
  };
};
Phase("Tel Hebron")
{
  Label("Charcoal");
  R_Combine("HB1-2")
  {
    R_Date("HB1", 3010, 35);
    R_Date("HB2", 2998, 23);
  };
};
```

```
};  
Phase("Tel Miqne IV")  
{  
  Label("Olive stones");  
  R_Combine("MQ1-2")  
  {  
    R_Date("MQ1", 2883, 26);  
    R_Date("MQ2", 2872, 27);  
  };  
};  
Phase("Tel Rehov D-4")  
{  
  Label("Olive stones");  
  R_Combine("R1, 2, GrN-26121 & GrN-18825")  
  {  
    R_Date("R1", 2845, 25);  
    R_Date("R2", 2913, 45);  
  };  
};  
Page( );  
Phase("Megiddo VIA destruction")  
{  
  Label("Seeds");  
  R_Combine("MG5-6")  
  {  
    R_Date("MG5", 2925, 25);  
    R_Date("MG6", 2864, 40);  
  };  
};  
Phase("Yoqne'am XVII")  
{  
  Label("Seeds");  
  R_Combine("Y1-2")  
  {  
    R_Date("Y1", 2866, 25);  
    R_Date("Y2", 2866, 33);  
  };  
  R_Combine("Y3-5")
```

```
{
  R_Date("Y3", 2776, 25);
  R_Date("Y4", 2817, 26);
  R_Date("Y5", 2818, 29);
};
R_Combine("Y6-7")
{
  R_Date("Y6", 2926, 30);
  R_Date("Y7", 2824, 30);
};
};
Phase("Tell Keisan 9a-b")
{
  Label("Charcoal");
  R_Combine("K5-6")
  {
    R_Date("K5", 2870, 35);
    R_Date("K6", 2842, 29);
  };
  R_Combine("K3, 4 & 7")
  {
    R_Date("K3", 2921, 31);
    R_Date("K4", 2870, 82);
    R_Date("K7", 2893, 50);
  };
};
};
Phase("Tell Qasile X")
{
  Label("Seeds");
  R_Combine("QS1-2")
  {
    R_Date("QS1", 2818, 26);
    R_Date("QS2", 2692, 24);
  };
  R_Combine("QS3-4")
  {
    R_Date("QS3", 2911, 26);
    R_Date("QS4", 2853, 25);
  };
};
};
```



```
};  
};  
};  
Boundary("Iron I/Iron IIA");  
Page( );  
Phase("Iron IIA")  
{  
  Phase("Rehov D-2")  
  {  
    Label("Olive stones");  
    R_Combine("R4-5")  
    {  
      R_Date("R4", 2757, 20);  
      R_Date("R5", 2760, 40);  
    };  
  };  
  Phase("Rehov E-1b")  
  {  
    Label("Olive stones");  
    R_Combine("R6-7")  
    {  
      R_Date("R6", 2685, 25);  
      R_Date("R7", 2678, 20);  
    };  
  };  
  Phase("Megiddo H5")  
  {  
    R_Combine("MG13-14")  
    {  
      R_Date("MG13", 2796, 28);  
      R_Date("MG14", 2825, 25);  
    };  
  };  
  Phase("Yoqne'am XIVb")  
  {  
    Label("Charcoal");  
    R_Combine("Y8-10")  
    {
```

```
R_Date("Y8", 2649, 31);
R_Date("Y9", 2725, 25);
R_Date("Y10", 2739, 35);
};
};
Phase("Horbat Rosh Zayit Ila")
{
  Label("Seeds");
  R_Combine("RZ1,2 & 6")
  {
    R_Date("RZ1", 2745, 30);
    R_Date("RZ2", 2755, 22);
    R_Date("RZ6", 2689, 28);
  };
  R_Combine("RZ3-5")
  {
    R_Date("RZ3", 2745, 30);
    R_Date("RZ4", 2729, 37);
    R_Date("RZ5", 2692, 31);
  };
};
Phase("Hazor XA")
{
  Label("Charcoal");
  R_Combine("HZ13-14")
  {
    R_Date("HZ13", 2700, 27);
    R_Date("HZ14", 2777, 24);
  };
};
Phase("Hazor IXA")
{
  Label("Olive stones");
  R_Combine("HZ15-16")
  {
    R_Date("HZ15", 2697, 24);
    R_Date("HZ16", 2689, 27);
  };
};
```

```
};  
};  
Boundary("End");  
};  
};
```

B1

```
Options()  
{  
  Resolution=1;  
};  
Plot()  
{  
  Sequence()  
  {  
    Boundary("Start");  
    Phase("LBA/IAI")  
    {  
      Phase("Megiddo K-6")  
      {  
        Label("Olive stones");  
        R_Combine("MG1-2")  
        {  
          R_Date("MG1", 2893, 27);  
          R_Date("MG2", 2894, 23);  
        };  
        R_Combine("MG3-4")  
        {  
          R_Date("MG3", 2968, 30);  
          R_Date("MG4", 2918, 22);  
        };  
      };  
    };  
    Phase("Tell Keisan 13")  
    {  
      Label("Charcoal");  
      R_Combine("K1-2")
```

```
{
  R_Date("K1", 2999, 29);
  R_Date("K2", 2984, 20);
};
};
Phase("Hazor XII/XI")
{
  Label("Charcoal");
  R_Combine("HZ1 & 6")
  {
    R_Date("HZ1", 2945, 50);
    R_Date("HZ6", 2975, 35);
  };
  R_Combine("HZ2 & 7")
  {
    R_Date("HZ2", 2965, 50);
    R_Date("HZ7", 2940, 30);
  };
  R_Combine("HZ4 & 9")
  {
    R_Date("HZ4", 3650, 50);
    R_Date("HZ9", 3570, 53);
  };
  R_Combine("HZ5 & 10")
  {
    R_Date("HZ5", 3370, 60);
    R_Date("HZ10", 3375, 30);
  };
  Label("Olive stones");
  R_Combine("HZ3 & 8")
  {
    R_Date("HZ3", 3060, 50);
    R_Date("HZ8", 3060, 30);
  };
};
};
Phase("Tel Hebron")
{
  Label("Charcoal");
```

```
R_Combine("HB1-2")
{
  R_Date("HB1", 3010, 35);
  R_Date("HB2", 2998, 23);
};
};
Phase("Tel Migne IV")
{
  Label("Olive stones");
  R_Combine("MQ1-2")
  {
    R_Date("MQ1", 2883, 26);
    R_Date("MQ2", 2872, 27);
  };
};
Phase("Tel Rehov D-4")
{
  Label("Olive stones");
  R_Combine("R1, 2, GrN-26121 & GrN-18825")
  {
    R_Date("R1", 2845, 25);
    R_Date("R2", 2913, 45);
    R_Date("GrN-26121", 2890, 30);
    R_Date("GrN-18825", 2870, 50);
  };
};
Page( );
Phase("Shiloh V")
{
  Label("Charred grain");
  R_Date("SH1", 2868, 20);
  R_Date("SH2", 2854, 25);
  Label("Charred raisins");
  R_Date("SH3", 2897, 23);
  Label("Charred seeds");
  R_Date("SH4", 2959, 28);
};
Phase("Megiddo VIA pre-destruction")
```

```
{
  R_Date("MG7",2880,30);
  R_Date("MG8",2910,25);
};
Phase("Megiddo VIA destruction")
{
  Label("Seeds");
  R_Combine("MG5-6")
  {
    R_Date("MG5", 2925, 25);
    R_Date("MG6", 2864, 40);
  };
  Label("Olive stones");
  R_Date("MG9",2760,26);
  R_Date("MG10",2765,25);
  R_Date("MG11",2845,25);
  R_Date("MG12",2855,25);
};
Phase("Beams in Megiddo VIA destruction")
{
  Label("Charcoal");
  R_Date("MG17", 2895, 25);
  R_Date("MG18", 2845, 45);
  R_Date("MG19", 2890, 25);
  R_Date("MG20", 2825, 25);
  R_Date("MG21", 2830, 20);
  R_Date("MG22", 2805, 25);
  R_Date("MG23", 2870, 20);
  R_Date("MG24", 2820, 45);
  R_Date("MG25", 2850, 20);
  R_Date("MG26", 2875, 20);
  R_Date("MG27", 2955, 20);
  R_Date("MG30", 2865, 55);
  R_Date("MG31", 2775, 25);
};
Phase("Yoqne'am XVII")
{
  Label("Seeds");
```



```
R_Combine("Y1-2")
{
  R_Date("Y1", 2866, 15);
  R_Date("Y2", 2866, 33);
};
R_Combine("Y3-5")
{
  R_Date("Y3", 2776, 15);
  R_Date("Y4", 2817, 26);
  R_Date("Y5", 2818, 29);
};
R_Combine("Y6-7")
{
  R_Date("Y6", 2926, 30);
  R_Date("Y7", 2824, 30);
};
R_Combine("Y11-13")
{
  R_Date("Y11", 2925, 38);
  R_Date("Y12", 2897, 38);
  R_Date("Y13", 2929, 54);
};
Phase("Tell Keisan 9a-b")
{
  Label("Charcoal");
  R_Combine("K5-6")
  {
    R_Date("K5", 2870, 35);
    R_Date("K6", 2842, 29);
  };
  R_Combine("K3, 4 & 7")
  {
    R_Date("K3", 2921, 31);
    R_Date("K4", 2870, 82);
    R_Date("K7", 2893, 35);
  };
  R_Date("K8", 2855, 29);
```

```
R_Date("K9", 2674, 30);
};
Phase("Tell Qasile X")
{
  Label("Seeds");
  R_Combine("QS1-4")
  {
    R_Date("QS1", 2818, 26);
    R_Date("QS2", 2692, 24);
    R_Date("QS3", 2911, 26);
    R_Date("QS4", 2853, 25);
  };
  R_Combine("QS9-11")
  {
    R_Date("QS9", 2864, 40);
    R_Date("QS10", 2818, 38);
    R_Date("QS11", 2897, 44);
  };
  R_Date("QS5", 2895, 25);
  R_Date("QS6", 2753, 22);
  R_Date("QS7", 2800, 25);
  R_Date("QS8", 2882, 28);
};
Phase("Tel Dor")
{
  R_Date("D1", 2803, 16);
  R_Date("D2", 2783, 22);
};
Phase("Tel Hadar IV")
{
  R_Date("HD1", 2791, 52);
  R_Date("HD2", 2853, 13);
};
Phase("Tel Rehov D-3")
{
  Label("Olive stones");
  R_Combine("R3")
  {
```

```
R_Date("R3a", 2800, 20);
R_Date("GrN-19033", 2835, 45);
R_Date("GrN-26119", 2720, 30);
};
};
};
Boundary("Iron I/Iron IIA");
Page( );
Phase("Iron IIA")
{
Phase("Rehov D-2")
{
Label("Olive stones");
R_Combine("R4, 5 & GrN-26112")
{
R_Date("R4", 2757, 20);
R_Date("R5", 2770, 23);
R_Date("GrN-26112", 2805, 15);
};
};
Phase("Rehov E-1b/E-1823")
{
Label("Olive stones");
R_Combine("R6-7")
{
R_Date("R6", 2685, 25);
R_Date("R7", 2678, 20);
};
R_Date("R8",2754,24);
};
Phase("Aphek X-8")
{
R_Date("A1",2667,20);
};
Phase("Tel Dor D28b/c")
{
R_Date("D3",2757,18);
R_Date("D4",2764,22);
```

```
R_Date("D5",2779,24);
R_Date("D6",2750,23);
};
Phase("Megiddo H5")
{
  R_Combine("MG13-14")
  {
    R_Date("MG13",2783,32);
    R_Date("MG14",2859,34);
  };
  R_Date("MG15",2695,50);
  R_Date("MG16",2770,80);
};
Phase("Yoqne'am XIVb")
{
  Label("Charcoal");
  R_Combine("Y8-10")
  {
    R_Date("Y8", 2649, 31);
    R_Date("Y9", 2725, 25);
    R_Date("Y10", 2739, 35);
  };
};
Phase("Horbat Rosh Zayit IIa")
{
  Label("Seeds");
  R_Combine("RZ1,2 & 6")
  {
    R_Date("RZ1", 2745, 30);
    R_Date("RZ2", 2755, 22);
    R_Date("RZ6", 2689, 28);
  };
  R_Combine("RZ3-5")
  {
    R_Date("RZ3", 2745, 30);
    R_Date("RZ4", 2729, 37);
    R_Date("RZ5", 2692, 31);
  };
};
```

```
R_Date("RZ7", 2709,15);
};
Phase("Bethsaida VI")
{
  Label("Seeds");
  R_Combine("4281")
  {
    R_Date("BD1", 2820, 35);
    R_Date("BD2", 2786, 25);
  };
};
Phase("Hazor XA")
{
  Label("Charcoal");
  R_Combine("HZ13-14")
  {
    R_Date("HZ13", 2700, 27);
    R_Date("HZ14", 2777, 24);
  };
};
Phase("Hazor IXA")
{
  Label("Olive stones");
  R_Combine("HZ15-16")
  {
    R_Date("HZ15", 2697, 24);
    R_Date("HZ16", 2689, 27);
  };
};
Phase("Tel el-Hammah middle phase")
{
  R_Date("HM3",2815,29);
  R_Date("HM4",2675,23);
  R_Date("HM5",2688,25);
  R_Date("HM6",2687,20);
  R_Date("HM7",2701,22);
  R_Date("HM8",2609,21);
  R_Date("HM9",2587,23);
```

```
R_Date("HM10",2634,23);
R_Date("HM11",2636,23);
R_Date("HM12",2722,24);
R_Date("HM13",2728,28);
};
Phase("Tell es-Safi IV")
{
R_Date("SF1",2661,30);
R_Date("SF2",2723,18);
};
Phase("Negev Highlands")
{
R_Date("NH1", 2930, 30);
R_Date("NH2", 2840, 15);
};
};
Boundary("End");
};
};
```

C1

```
Options( )
{
Resolution=1;
};
Plot( )
{
Sequence("Main")
{
Boundary("Start");
Phase("LBA/IAI")
{
Phase("Megiddo K-6")
{
Label("Olive stones");
R_Combine("MG1-2")
{
```

```
R_Date("MG1", 2893, 27);
R_Date("MG2", 2894, 23);
};
R_Combine("MG3-4")
{
  R_Date("MG3", 2968, 30);
  R_Date("MG4", 2918, 22);
};
};
Phase("Tell Keisan 13")
{
  Label("Charcoal");
  R_Combine("K1-2")
  {
    R_Date("K1", 2999, 29);
    R_Date("K2", 2984, 20);
  };
};
Phase("Hazor XII/XI")
{
  Label("Charcoal");
  R_Combine("HZ1 & 6")
  {
    R_Date("HZ1", 2945, 50);
    R_Date("HZ6", 2975, 35);
  };
  R_Combine("HZ2 & 7")
  {
    R_Date("HZ2", 2965, 50);
    R_Date("HZ7", 2940, 30);
  };
  R_Combine("HZ4 & 9")
  {
    R_Date("HZ4", 3650, 50);
    R_Date("HZ9", 3570, 53);
  };
  R_Combine("HZ5 & 10")
  {
```

```
R_Date("HZ5", 3370, 60);
R_Date("HZ10", 3375,30);
};
Label("Olive stones");
R_Combine("HZ3 & 8")
{
  R_Date("HZ3", 3060, 50);
  R_Date("HZ8", 3060, 30);
};
};
Phase("Tel Hebron")
{
  Label("Charcoal");
  R_Combine("HB1-2")
  {
    R_Date("HB1", 3010, 35);
    R_Date("HB2", 2998, 23);
  };
};
Phase("Tel Miqne IV")
{
  Label("Olive stones");
  R_Combine("MQ1-2")
  {
    R_Date("MQ1", 2883, 26);
    R_Date("MQ2", 2872, 27);
  };
};
Phase("Tel Rehov D-4")
{
  Label("Olive stones");
  R_Combine("R1, 2, GrN-26121 & GrN-18825")
  {
    R_Date("R1", 2845, 25);
    R_Date("R2", 2913, 45);
    R_Date("GrN-26121", 2890, 30);
    R_Date("GrN-18825", 2870, 50);
  };
};
```



```
};  
Page( );  
Phase("Shiloh V")  
{  
  Label("Charred grain");  
  R_Date("SH1", 2868, 20);  
  R_Date("SH2", 2854, 25);  
  Label("Charred raisins");  
  R_Date("SH3", 2897, 23);  
  Label("Charred seeds");  
  R_Date("SH4", 2959, 28);  
};  
};  
Boundary("Iron I/IIA");  
Page( );  
Phase("Iron IIA")  
{  
  Phase("Rehov D-2")  
  {  
    Label("Olive stones");  
    R_Combine("R4, 5 & GrN-26112")  
    {  
      R_Date("R4", 2757, 20);  
      R_Date("R5", 2770, 23);  
      R_Date("GrN-26112", 2805, 15);  
    };  
  };  
  Phase("Rehov E-1b/E-1823")  
  {  
    Label("Olive stones");  
    R_Combine("R6-7")  
    {  
      R_Date("R6", 2685, 25);  
      R_Date("R7", 2678, 20);  
    };  
    R_Date("R8", 2754, 24);  
  };  
  Phase("Aphek X-8")
```

```
{
  R_Date("A1",2667,20);
};
Phase("Tell Dor D28b/c")
{
  R_Date("D3",2757,18);
  R_Date("D4",2764,22);
  R_Date("D5",2779,24);
  R_Date("D6",2750,23);
};
Phase("Megiddo H5")
{
  R_Combine("MG13-14")
  {
    R_Date("MG13",2783,32);
    R_Date("MG14",2859,34);
  };
  R_Date("MG15",2695,50);
  R_Date("MG16",2770,80);
};
Phase("Yoqne'am XIVb")
{
  Label("Charcoal");
  R_Combine("Y8-10")
  {
    R_Date("Y8", 2649, 31);
    R_Date("Y9", 2725, 25);
    R_Date("Y10", 2739, 35);
  };
};
Phase("Horbat Rosh Zayit IIa")
{
  Label("Seeds");
  R_Combine("RZ1,2 & 6")
  {
    R_Date("RZ1", 2745, 30);
    R_Date("RZ2", 2755, 22);
    R_Date("RZ6", 2689, 28);
  };
};
```

```
};
R_Combine("RZ3-5")
{
  R_Date("RZ3", 2745, 30);
  R_Date("RZ4", 2729, 37);
  R_Date("RZ5", 2692, 31);
};
R_Date("RZ7", 2709,15);
};
Phase("Bethsaida VI")
{
  Label("Seeds");
  R_Combine("4281")
  {
    R_Date("BD1", 2820, 35);
    R_Date("BD2", 2786, 25);
  };
};
Phase("Hazor XA")
{
  Label("Charcoal");
  R_Combine("HZ13-14")
  {
    R_Date("HZ13", 2700, 27);
    R_Date("HZ14", 2777, 24);
  };
};
Phase("Hazor IXA")
{
  Label("Olive stones");
  R_Combine("HZ15-16")
  {
    R_Date("HZ15", 2697, 24);
    R_Date("HZ16", 2689, 27);
  };
};
Phase("Tel el-Hammah middle phase")
{
```

```
R_Date("HM3",2815,29);
R_Date("HM4",2675,23);
R_Date("HM5",2688,25);
R_Date("HM6",2687,20);
R_Date("HM7",2701,22);
R_Date("HM8",2609,21);
R_Date("HM9",2587,23);
R_Date("HM10",2634,23);
R_Date("HM11",2636,23);
R_Date("HM12",2722,24);
R_Date("HM13",2728,28);
};
Phase("Tell es-Safi IV")
{
R_Date("SF1",2661,30);
R_Date("SF2",2723,18);
};
Phase("Negev Highlands")
{
R_Date("NH1", 2930, 30);
R_Date("NH2", 2840, 15);
};
};
Boundary("End");
};
Sequence("Late Iron I")
{
Boundary();
Phase("Late Iron I")
{
Phase("Megiddo VIA pre-destruction")
{
R_Date("MG7",2880,30);
R_Date("MG8",2910,25);
};
Phase("Megiddo VIA destruction")
{
Label("Seeds");
```

```
R_Combine("MG5-6")
{
  R_Date("MG5", 2925, 25);
  R_Date("MG6", 2864, 40);
};
Label("Olive stones");
R_Date("MG9", 2760, 26);
R_Date("MG10", 2765, 25);
R_Date("MG11", 2845, 25);
R_Date("MG12", 2855, 25);
};
Phase("Beams in Megiddo VIA destruction")
{
  Label("Charcoal");
  R_Date("MG17", 2895, 25);
  R_Date("MG18", 2845, 45);
  R_Date("MG19", 2890, 25);
  R_Date("MG20", 2825, 25);
  R_Date("MG21", 2830, 20);
  R_Date("MG22", 2805, 25);
  R_Date("MG23", 2870, 20);
  R_Date("MG24", 2820, 45);
  R_Date("MG25", 2850, 20);
  R_Date("MG26", 2875, 20);
  R_Date("MG27", 2955, 20);
  R_Date("MG30", 2865, 55);
  R_Date("MG31", 2775, 25);
};
Phase("Yoqne'am XVII")
{
  Label("Seeds");
  R_Combine("Y1-2")
  {
    R_Date("Y1", 2866, 15);
    R_Date("Y2", 2866, 33);
  };
  R_Combine("Y3-5")
  {
```

```

R_Date("Y3", 2776, 15);
R_Date("Y4", 2817, 26);
R_Date("Y5", 2818, 29);
};
R_Combine("Y6-7")
{
R_Date("Y6", 2926, 30);
R_Date("Y7", 2824, 30);
};
R_Combine("Y11-13")
{
R_Date("Y11", 2925, 38);
R_Date("Y12", 2897, 38);
R_Date("Y13", 2929, 54);
};
};
Phase("Tell Keisan 9a-b")
{
Label("Charcoal");
R_Combine("K5-6")
{
R_Date("K5", 2870, 35);
R_Date("K6", 2842, 29);
};
R_Combine("K3, 4 & 7")
{
R_Date("K3", 2921, 31);
R_Date("K4", 2870, 82);
R_Date("K7", 2893, 35);
};
R_Date("K8", 2855, 29);
R_Date("K9", 2674, 30);
};
Phase("Tell Qasile X")
{
Label("Seeds");
R_Combine("QS1-2")
{

```

```
R_Date("QS1", 2818, 26);
R_Date("QS2", 2692, 24);
};
R_Combine("QS3-4")
{
  R_Date("QS3", 2911, 26);
  R_Date("QS4", 2853, 25);
  R_Date("QS9", 2864, 40);
  R_Date("QS10", 2818, 38);
  R_Date("QS11", 2897, 44);
};
R_Date("QS5", 2895, 25);
R_Date("QS6", 2753, 22);
R_Date("QS7", 2800, 25);
R_Date("QS8", 2882, 28);
};
Phase("Tel Dor")
{
  R_Date("D1", 2803, 16);
  R_Date("D2", 2783, 22);
};
Phase("Tel Hadar IV")
{
  R_Date("HD1", 2791, 52);
  R_Date("HD2", 2853, 13);
};
Phase("Tel Rehov D-3")
{
  Label("Olive stones");
  R_Combine("R3")
  {
    R_Date("R3a", 2800, 20);
    R_Date("GrN-19033", 2835, 45);
    R_Date("GrN-26119", 2720, 30);
  };
};
};
Boundary("=Iron I/Iron IIA");
```

```
};  
};
```

D1

```
Options(  
{  
  Resolution=1;  
});  
Plot(  
{  
  Sequence("Main sequence")  
  {  
    Boundary( );  
    Phase("Megiddo K-6")  
    {  
      Label("Olive stones");  
      R_Combine("MG1-2")  
      {  
        R_Date("MG1", 2893, 27);  
        R_Date("MG2", 2894, 23);  
      };  
      R_Combine("MG3-4")  
      {  
        R_Date("MG3", 2968, 30);  
        R_Date("MG4", 2918, 22);  
      };  
    };  
    Boundary( );  
    Phase("Megiddo VIA pre-destruction")  
    {  
      R_Date("MG7",2880,30);  
      R_Date("MG8",2910,25);  
    };  
    Boundary( );  
    Phase("Megiddo VIA destruction")  
    {
```



```
Label("Seeds");
R_Combine("MG5-6")
{
  R_Date("MG5", 2925, 25);
  R_Date("MG6", 2864, 40);
};
Label("Olive stones");
R_Date("MG9",2760,26);
R_Date("MG10",2765,25);
R_Date("MG11",2845,25);
R_Date("MG12",2855,25);
};
Boundary("Iron I/Iron IIA");
Phase("K3/H6");
Boundary();
Phase("Megiddo H5")
{
  R_Combine("MG13-14")
  {
    R_Date("MG13", 2796, 28);
    R_Date("MG14", 2825, 25);
  };
  R_Date("MG15",2695,50);
};
Boundary( );
};
Sequence("Charred beams")
{
  Tau_Boundary( );
  Phase("Beams in Megiddo VIA destruction")
  {
    Label("Charcoal");
    R_Date("MG17", 2895, 25);
    R_Date("MG18", 2845, 45);
    R_Date("MG19", 2890, 25);
    R_Date("MG20", 2825, 25);
    R_Date("MG21", 2830, 20);
    R_Date("MG22", 2805, 25);
```

```
R_Date("MG23", 2870, 20);
R_Date("MG24", 2820, 45);
R_Date("MG25", 2850, 20);
R_Date("MG26", 2875, 20);
R_Date("MG27", 2955, 20);
R_Date("MG30", 2865, 55);
R_Date("MG31", 2775, 25);
};
Boundary("=Iron I/Iron IIA");
};
};
```

D2

```
Options( )
{
  Resolution=1;
};
Plot( )
{
  Sequence("Main sequence")
  {
    Boundary( );
    Phase("Megiddo K-6")
    {
      Label("Olive stones");
      R_Combine("MG1-2")
      {
        R_Date("MG1", 2893, 27);
        R_Date("MG2", 2894, 23);
      };
      R_Combine("MG3-4")
      {
        R_Date("MG3", 2968, 30);
        R_Date("MG4", 2918, 22);
      };
    };
  };
  Boundary( );
```

```
Phase("Megiddo VIA pre-destruction")
{
  R_Date("MG7",2880,30);
  R_Date("MG8",2910,25);
};
Boundary( );
Phase("Megiddo VIA destruction")
{
  Label("Seeds");
  R_Combine("MG5-6")
  {
    R_Date("MG5", 2925, 25);
    R_Date("MG6", 2864, 40);
  };
  Label("Olive stones");
  R_Date("MG9",2760,26);
  R_Date("MG10",2765,25);
  R_Date("MG11",2845,25);
  R_Date("MG12",2855,25);
};
Boundary("Iron I/iron IIA");
Phase("K3/H6");
Boundary( );
Phase("Megiddo H5")
{
  R_Combine("MG13-14")
  {
    R_Date("MG13", 2796, 28);
    R_Date("MG14", 2825, 25);
  };
  R_Date("MG15",2695,50);
};
Boundary( );
};
```